Fundamental limitations on photoisomerization from thermodynamic resource theories

Nicole Yunger Halpern and David T. Limmer

Phys. Rev. A **101**, 042116 — Published 17 April 2020

DOI: 10.1103/PhysRevA.101.042116

Fundamental limitations on photoisomerization from thermodynamic resource theories

Nicole Yunger Halpern[1, 2, 3, 4, 5] and David T. Limmer[6, 7, 8]

[1] *Institute for Quantum Information and Matter, California Institute of Technology, Pasadena, CA 91125, USA*
[2] *Kavli Institute for Theoretical Physics, University of California, Santa Barbara, CA 93106, USA*
[3] *ITAMP, Harvard-Smithsonian Center for Astrophysics, Cambridge, MA 02138, USA*
[4] *Department of Physics, Harvard University, Cambridge, MA 02138, USA*
[5] *Research Laboratory of Electronics, Massachusetts Institute of Technology, Cambridge, Massachusetts 02139, USA*
[6] *Department of Chemistry, University of California, Berkeley, CA 94720, USA*
[7] *Kavli Energy NanoSciences Institute, University of California, Berkeley, CA 94720, USA*
[8] *Lawrence Berkeley National Laboratory, University of California, Berkeley, CA 94720, USA*

(Dated: March 11, 2020)

Small, out-of-equilibrium, and quantum systems defy simple thermodynamic expressions. Such systems are exemplified by molecular switches, which exchange heat with a bath. These molecules can photoisomerize, or change conformation, or switch, upon absorbing light. The photoisomerization probability depends on kinetic details that couple the molecule's energetics to its dissipation. Therefore, a simple, general, thermodynamic-style bound on the photoisomerization probability seems out of reach. We derive such a bound using a resource theory. The resource-theory framework is a set of mathematical tools, developed in quantum information theory, used to generalize thermodynamics to small and quantum settings. From this toolkit has been derived a generalization of the second law, the thermomajorization preorder. We use thermomajorization to upper-bound the photoisomerization probability. Then, we compare the bound with an equilibrium prediction and with Lindbladian model. We identify a realistic parameter regime in which the Lindbladian evolution saturates the thermomajorization bound. We also quantify the energy coherence in the electronic degree of freedom, and we argue that this coherence cannot promote photoisomerization. This work illustrates how quantum-information-theoretic thermodynamics can elucidate complex quantum processes in nature, experiments, and synthetics.

Thermodynamics quantifies ideal processes with simple expressions and constrains processes that deviate from the ideal. This simplicity vanishes in the face of small systems and intermediate time scales. Such realistic settings yoke work, heat, and entropy production to kinematic details, exposing each as a fluctuating quantity. Yet one can hope to bound kinematic results with general thermodynamic-style expressions. Such results have enjoyed theoretical and experimental success. For example, fluctuation theorems and Jarzynski's equality [1–3] constrain ensembles of irreversible transformations. These results govern experiments, including with single molecules [4, 5], and information engines [6–8]. Additionally, thermodynamic uncertainty relations [9, 10] have constrained the precision with which microscopic currents can be generated. These findings have relevance to molecular motors [11, 12] and self-assembly [13, 14].

We derive general, thermodynamic-style statements about small far-from-equilibrium quantum systems: We derive bounds on molecular switches' photoisomerization, or switching driven by light. To do so, we leverage the quantum-information (QI) tool of thermodynamic resource theories.

Small molecules photoisomerize, or switch configurations, in many natural and synthetic systems [15–23]. Example photoisomers include retinal in rhodopsin, a pigment in the retina [24], and green fluorescent protein, a chromophore used throughout molecular imaging [25]. Three conveniences account for these molecular switches' prevalence. First, ultrafast femtosecond lasers offer control over photoisomerization [26–30]. Second, photoisomers can be synthesized easily. Third, one can easily encourage the expression of genes that code for isomers. Applications are widespread and include azobenzene-based solar-to-thermal fuels [31] and functional polymers [28, 32].

Despite their usefulness and prevalence, photoisomers are not understood completely: Experimental tools, such as time-resolved spectroscopy [33–36], expose only a subset of the relevant degrees of freedom (DOFs). Additionally, computational tools for simulating these processes remain under active development [37–45]. We will help remedy the deficiency using QI theory.

Figure 1 depicts a photoisomer and its energy landscape. Photoisomerization, or switching, begins with the molecule in its thermal state. The lowest electronic energy eigenstate approximates the room-temperature thermal state well. The heavy atoms' positions are parameterized with an angle φ. φ determines the electronic energy levels, because the electronic energy spacing far exceeds the energy spacings associated with the molecule's vibrations and rotations [46]. The ground electronic level exhibits two wells, centered near $\varphi = 0$ and $\varphi = \pi$. An energy barrier separates the well. $\varphi = 0, \pi$ define two conformations, or isomers, of the molecule: the *cis* and *trans* configurations. Low-lying excited electronic states can lack energy barriers. If excited by light, therefore, the molecule has the opportunity to change configurations while relaxing, in contact with its environment, to the lower electronic level. The

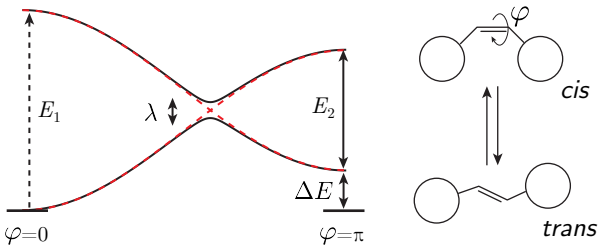

FIG. 1: Photoisomer's energy landscape and conformations. Two representative potential-energy surfaces for the ground and excited electronic states of an isomer, as well as the *cis* and *trans* configurations associated with the ground-state minima. The black curves represent adiabatic states, or instantaneous energy eigenstates. The red curves represent diabatic states, which approximately equal adiabatic states at $\varphi = 0, \pi$.

probability of changing conformation during relaxation is called the "photoisomerization yield."

The yield is difficult to predict for several reasons. First, dynamical factors determine the yield over intermediate time scales. These times exceed the time needed for the electronic DOF to relax to its ground state but are shorter than the time over which the whole molecule thermalizes. This intermediacy precludes straightforward thermodynamic statements. Second, the postexcitation evolution involves nonadiabaticity [47], dissipation [47], and rare bath fluctuations [48].

Hence studying the evolution computationally is difficult, and few general guiding principles exist.

We need a toolkit for deriving thermodynamic-style bounds on photoisomerization. These bounds should incorporate the coupling of quantum mechanical DOFs with small scales and thermal fluctuations. To construct such bounds, we turn to QI theory.

Resource theories are simple models developed in QI theory [49, 50]. They are relevant when restrictions constrain the processes that can occur, called "free operations," and the systems accessible, called "free systems." Consider, as an example, a thermodynamic setting in which systems exchange heat with a bath at a fixed temperature. The first law of thermodynamics constrains processes to conserve energy, and only thermal states can be accessed easily. The corresponding resource theory's free operations are called "thermal operations." All non-free systems, e.g., systems not in states thermal with respect to the environment's temperature, are "resources." Resources have value because they can fuel tasks such as work extraction. Resource theories originated to quantify entanglement and to clarify which QI-processing tasks entanglement could facilitate [51]. Since then, resource theories have been developed for other valuable quantities, including reference frames [52–57], randomness used in cryptography [49], coherence [58–60], "magic states" used in quantum computation [61], and thermodynamics [62–70].

Using a resource theory, one studies which systems R can transform into systems S under free operations ($R \mapsto S$); which cannot ($R \not\mapsto S$); how much of a resource W, such as work, is required to facilitate an otherwise impossible transformation ($R + W \mapsto S$ despite $R \not\mapsto S$); how many copies of S can be extracted from m copies of R; and what, generally, is possible and impossible. Results govern arbitrarily small systems and coherent quantum states. In thermodynamic resource theories, averaging in a large-system limit reproduces results consistent with expectations from statistical mechanics. Hence resource theories offer the potential for formulating sharp, general statements about complex, quantum systems. We harness this potential for molecules undergoing photoisomerization.

This paper is organized as follows. First, we review the resource theory that models heat exchanges. We then model the molecule within the resource theory (Sec. I). We bound the photoisomerization yield in two steps (Sec. II): First, we show that the electronic state's coherences relative to the energy eigenbasis cannot promote isomerization, if the environment is Markovian. This result enables us to bound the isomerization yield by focusing, second, on the density matrix's populations: We apply thermomajorization, a resource-theory result that generalizes the second law of thermodynamics. The yield is tightly constrained, we find, if the light source barely excites the molecule. If the light source fully excites the molecule to one high-energy eigenstate, thermomajorization's upper bound on the yield can be saturated.

We next quantify the coherences, relative to the energy eigenbasis, that the electronic state gains during photoisomerization (Sec. III). This coherence emerges after the molecule undergoes a dissipative Landau-Zener evolution, which we model within the resource theory. The model indicates that the molecule acts as a quantum clock [71–80]. An application of this coherence appears in the appendices, where work is shown to be extractable from the coherence. The Discussion concludes with this program's significance and opportunities (Sec. IV).

I. RESOURCE-THEORY MODEL FOR THE PHOTOISOMER

In this section, we review the resource theory that models heat exchanges. Then, we model the chemical problem within the resource theory: the molecule, bath, and light source in Sec. I A, followed by photoisomerization in Sec. I B. To specify a system in the resource theory, one specifies a tuple (ρ, H). The ρ denotes a quantum state, and the H denotes a Hamiltonian. Both are defined on a Hilbert space $\mathcal{H}$ of dimensionality d.

Each thermal operation consists of three steps: (i) A thermal system governed by an arbitrary Hamiltonian $H_\mathcal{B}$ is drawn from the bath at inverse temperature β: $(\rho_\mathcal{B} = \exp[-\beta H_\mathcal{B}]/Z_\mathcal{B},\ H_\mathcal{B})$, wherein $Z_\mathcal{B} := \mathrm{Tr}_\mathcal{B}[\exp(-\beta H_\mathcal{B})]$ denotes the partition function. (ii)

The system and bath interact via an arbitrary energy-conserving unitary U. (iii) A generalized environment $\mathcal{B}'$ is discarded. $\mathcal{B}'$ is often the bath, $\mathcal{B}$, but may be another subsystem. Mathematically, a thermal operation $\mathcal{T}$ is represented as

$$(\rho, H) \mapsto \mathcal{T}(\rho, H) \equiv \left(\mathrm{Tr}_{\mathcal{B}'} \left\{ U \left[\rho \otimes \rho_{\mathcal{B}} \right] U^\dagger \right\}, H \right). \quad (1)$$

The unitary satisfies a manifestation of the first law:

$$[U, H + H_{\mathcal{B}}] = 0. \quad (2)$$

The Hamiltonians are composed as $H + H_{\mathcal{B}} \equiv (H \otimes \mathbb{1}) + (\mathbb{1} \otimes H_{\mathcal{B}})$.

Only Eq. (2) restricts U. We do not assume that the system-bath interaction has any particular form or coupling strength; we assume only that (2) is satisfied. U can transfer arbitrary amounts of energy between the system and the bath in arbitrary times. To test our resource-theory results, we compare them with Lindblad models in Sections II D and III B. The Lindblad models involve more-specific couplings between the photoisomer and the bath. Such specific couplings are not required for most of our results. To model photoisomerization, we focus on an H that governs a photoisomer.

I A. Resource-theory model for the molecule, bath, and light source

Resource-theory model for the molecule: The angular DOF $\varphi \in [0, \pi]$ parameterizes the isomer's configuration and governs the electronic Hamiltonian [19]. We attribute to the molecule the Hamiltonian

$$H_{\mathrm{mol}} := \int_0^\pi d\varphi \, H_{\mathrm{mol}}(\varphi) \quad (3)$$
$$\equiv \int_0^\pi d\varphi \left[H_{\mathrm{elec}}(\varphi) \otimes |\varphi\rangle\langle\varphi| + \mathbb{1}_{\mathrm{elec}} \otimes \frac{\ell_\varphi^2}{2m} \right].$$

In each term in Eq. (3), the first factor acts on an electronic Hilbert space $\mathcal{H}_{\mathrm{elec}}$, and the second acts on a configurational Hilbert space $\mathcal{H}_\varphi$. $\mathbb{1}_{\mathrm{elec}}$ and $\mathbb{1}_\varphi$ denote the identity operators on $\mathcal{H}_{\mathrm{elec}}$ and on $\mathcal{H}_\varphi$. ℓ_φ denotes the angular-momentum operator associated with the quasiclassical mode φ, which has an effective mass m. The angular DOF is well-approximated as quasiclassical due to the chemical groups' sizes and masses [16]: The groups localize at angular coordinates far from the φ values at which $H_{\mathrm{elec}}(\varphi)$ is degenerate, satisfying the Born-Oppenheim approximation.

Our H_{mol} has the form of Hamiltonians in [66, 76]. There, a switch changes the system-of-interest Hamiltonian. φ acts as the switch here, and the electronic DOF acts as the system. A related model appeared very recently in [81].

The electronic Hamiltonian has the form in [19]:

$$H_{\mathrm{elec}}(\varphi) = \left[(2E_1 - \Delta E - E_2) \sin^2(\varphi/2) \right] |\psi_0\rangle\langle\psi_0| \quad (4)$$
$$+ \left[E_1 - (E_1 - \Delta E) \sin^2(\varphi/2) \right] |\psi_1\rangle\langle\psi_1|$$
$$+ \frac{\lambda}{2} (|\psi_0\rangle\langle\psi_1| + |\psi_1\rangle\langle\psi_0|) .$$

Figure 1 illustrates the energy landscape. The diabatic basis $\{|\psi_0\rangle, |\psi_1\rangle\}$ approximately diagonalizes the Hamiltonian at $\varphi = 0, \pi$. The constants $E_1, E_2, \Delta E > 0$ far exceed the interstate coupling $\lambda > 0$. The energy required to excite $|\psi_0\rangle|\varphi{=}0\rangle$ to $|\psi_1\rangle|\varphi{=}0\rangle$ is denoted by E_1. The energy of excitation from $|\psi_0\rangle|\varphi{=}\pi\rangle$ to $|\psi_1\rangle|\varphi{=}\pi\rangle$ is E_2. The energy stored during a transition from $|\psi_0\rangle|\varphi{=}0\rangle$ to $|\psi_0\rangle|\varphi{=}\pi\rangle$ is ΔE.

We notate the eigenenergies by $\mathcal{E}_\pm(\varphi)$, such that $\mathcal{E}_+(\varphi) \geq \mathcal{E}_-(\varphi)$, and the adiabatic basis by $\{|\mathcal{E}_\pm(\varphi)\rangle\}$:

$$H_{\mathrm{elec}}(\varphi) = \sum_{\mu=\pm} \mathcal{E}_\mu(\varphi) |\mathcal{E}_\mu(\varphi)\rangle\langle\mathcal{E}_\mu(\varphi)|. \quad (5)$$

Though simple, this single-mode model reproduces linear and time-dependent spectroscopy of photoswitches like rhodopsin. The model also accounts for high reaction efficiencies [82]. Furthermore, the model captures the photoisomerization yield's dependence on environmental factors [19, 83, 84]. Consequently, models of the form of Eq. 4 are routinely studied to explore environmental effects [85, 86] and to benchmark novel numerical techniques [30, 87–89].

Resource-theory model for the bath: A Hamiltonian $H_{\mathcal{B}} = \sum_k \mathscr{E}_k |\mathscr{E}_k\rangle\langle\mathscr{E}_k|$ governs the bath, which occupies a Gibbs state $\rho_{\mathcal{B}} = \sum_k \exp(-\beta\mathscr{E}_k)/Z_{\mathcal{B}} |\mathscr{E}_k\rangle\langle\mathscr{E}_k|$. We assume that $H_{\mathcal{B}}$ has the properties in [66, Suppl. Note 1, p. 5], invoking the justifications therein. For example, degeneracies are assumed to grow exponentially with energy.

Resource-theory model for the light source: A laser or sunlight performs work on the molecule [70, 75, 90–92]. We model the light as a multimode bosonic field in a state ρ_{laser}. Examples include coherent states, but ρ_{laser} can have an arbitrary form. ρ_{laser} dictates to which states the molecule can be photoexcited, and our results hold for arbitrary photoexcited states. We consider a range of photoexcited states (Sections II C and II D) and so a range of ρ_{laser}'s.

We denote the oscillator Hamiltonian, H_{laser}, and expand it in particle-number states $|n_\omega\rangle$ that satisfy the eigenvalue equation $N_\omega |n_\omega\rangle = n_\omega |n_\omega\rangle$, wherein $n_\omega = 0, 1, 2, \ldots$ Our arguments do not rely on the precise form of the density of states.

Each fixed-ω term resembles the ladder Hamiltonians with which batteries have been modeled in thermodynamic resource theories [68, 75, 93–95]. Batteries are often modeled with spectra unbounded from below, because ground states can complicate accountings of coherence [75, 96]. H_{laser} has a ground state, modeling a real physical Hamiltonian. However, the ground state will lack much population. Hence comparing the light source with resource-theory batteries is justified.

I B. Resource-theory model for photoisomerization

The molecule begins in thermal equilibrium with the bath,[1] in the state $\rho = \exp(-\beta H_{\rm mol})/Z_{\rm mol}$. This state follows from long-time thermalization. We will focus on the molecule's later rotation, which happens over a short time and can break the weak-coupling assumption that leads to thermal states. We assume that Eq. 4 is parameterized such that the *cis* isomer is strongly energetically preferred [19]: $\rho \approx |\psi_0\rangle\langle\psi_0| \otimes |\varphi{=}0\rangle\langle\varphi{=}0|$. Our results analogously govern isomers whose *trans* states are preferred, such as azobenzene.

We model photoisomerization with three thermal operations, represented by arrows $\mapsto$. First, the laser excites the molecule,

$$e^{-\beta H_{\rm mol}}/Z_{\rm mol} \otimes \rho_{\rm laser} \mapsto \rho_{\rm i} \otimes |\varphi{=}0\rangle\langle\varphi{=}0| \, , \qquad (6)$$

at the angular coordinate $\varphi = 0$. The laser forms part of the generalized environment $\mathcal{B}'$ traced out in Eq. (1). $\rho_{\rm i}$ denotes the new electronic state, which depends on $\rho_{\rm laser}$ and on the thermal operation's form (on how the molecule couples to the bath and the laser). Our calculations are evaluated on a range of $\rho_{\rm i}$'s, from fully to barely excited (Sections II C and II D). Second, the molecule rotates:

$$\rho_{\rm i} \otimes |\varphi{=}0\rangle\langle\varphi{=}0| \mapsto \rho_{\rm f}. \qquad (7)$$

$\rho_{\rm f}$ denotes the post-photoisomerization state. Most of its weight lies on the *trans* states, for which $\varphi = \pi$. Maximizing the isomerization yield amounts to maximizing the final state's weight on the lower *trans* level,

$$\rho_-(\pi) := \langle \mathcal{E}_-(\pi), \varphi{=}\pi | \rho_{\rm f} | \mathcal{E}_-(\pi), \varphi{=}\pi \rangle. \qquad (8)$$

Third, the molecule thermalizes to $\exp(-\beta H_{\rm mol})/Z_{\rm mol}$.

Appendix B 2 details a more sophisticated model for step 2: The thermal operation (7) is decomposed as a sequence of thermal operations. The angular DOF φ serves as a quantum clock [71–80] as the molecule rotates at some speed v. This sequence models a dissipative Landau-Zener transition. The sophisticated model (of a sequence of thermal operations) is consistent with the simpler model (of one thermal operation): Every composition of thermal operations is a thermal operation (App. A). Every thermal operation—including every composite—obeys thermomajorization. To test our resource-theory results, we compare them with specific minimal models in Sections II D and III B. The models models involve specific Lindbladian couplings between the photoisomer and the bath. However, duch specific couplings are not required for most of our results.

[1] In certain cases, the molecule may begin out of equilibrium [16, 21, 23]. A source of work and/or coherence keeps the molecule from thermalizing. This resource can straightforwardly be incorporated into our model. Such a resource would affect the postexcitation states accessible to the molecule (the right-hand side of Eq. (6)). Our main result, the thermomajorization bound on the photoisomerization yield, governs arbitrary postexcitation states. Hence a nonequilibrium initial state does not affect our result's form.

II. LIMITATIONS ON PHOTOISOMERIZATION YIELD

The rotational thermal operation (7) leaves the photoisomer in a state $\rho_{\rm f}$. We upper-bound the isomerization yield $\rho_-(\pi)$ in two steps. First, we show that the electronic state's coherences relative to the energy eigenbasis cannot affect the yield (Sec. II A). This result relies on the independence of coherences' and populations' evolutions under thermal operations [90, 97]. The coherences' irrelevance enable us to bound the yield by focusing on density matrices' populations. The populations' evolutions are constrained by thermomajorization, a preorder that generalizes the second law of thermodynamics [63, 66, 98–104]. We review thermomajorization (Sec. II B), then apply it to bound the photoisomerization yield (Sec. II C). To evaluate the bound's tightness, we compare with Lindblad evolution (Sec. II D). The bound is tight, we find, when kinetic parameters favor photoisomerization.

II A. Electronic energy coherences cannot influence the photoisomerization yield

In conventional thermodynamics, a system's free energy declines monotonically under spontaneous processes. Resource-theory monotones behave similarly. A monotone is a function f, evaluated on a system (ρ, H), that decreases monotonically under free operations [50, 67, 104]: $f(\rho, H) \geq f(\mathcal{T}(\rho, H))$. Monotones quantify resourcefulness, which is eroded monotonically by free operations, i.e., thermalization. Different monotones quantify the system's ability to fuel different tasks, such as work extraction and timekeeping.

Coherence can be grouped into modes, each associated with one energy gap [90, 97]. Let $H = \sum_j E_j |j\rangle\langle j|$ denote a Hamiltonian that governs a state ρ. The ω mode of H consists of the pairs (j, k) whose gaps $|E_j - E_k| = \omega$. If $\rho_{jk} := \langle j|\rho|k\rangle$, then ρ_{jk} encodes coherence when $j \neq k$. A state's mode-ω coherence has been quantified with the one-norm [90], defined as $||A||_1 := {\rm Tr}\left(\sqrt{AA^\dagger}\right)$ for a matrix A. Suppose that some thermal operation $\mathcal{T}$ maps (ρ, H) to (σ, H). The modes' one-norms decay monotonically and independently [90, 97]:

$$\sum_{j,k:|E_j - E_k| = \omega} ||\rho_{jk}||_1 \geq \sum_{j,k:|E_j - E_k| = \omega} ||\sigma_{jk}||_1 \quad \forall \omega. \qquad (9)$$

The modes' independence follows from thermal operations' commuting with time translations. We review the

proof in App. B. This result relies on sequential thermal operations' modeling interactions with a Markovian bath. Markovianity is a common assumption that models rhodopsin's photoisomerization [105].

The molecule's $H_{\rm elec}(0)$ has a coherence mode $\omega_1 = \mathcal{E}_+(0) - \mathcal{E}_-(0) = E_1$ and a population mode $\omega_0 = 0$. The initial state $\approx |\mathcal{E}_-(0)\rangle$ lacks coherence, so the laser provides all the coherence in the photoexcited state $\rho_{\rm i}$. Suppose, for example, that the laser creates an even superposition, $\frac{1}{\sqrt{2}}\left(|\mathcal{E}_-(0)\rangle + |\mathcal{E}_+(0)\rangle\right)|\varphi{=}0\rangle$, as in Fig. 2b). Photoexcitation gives the state a nonzero amount

$$\left|\left| \sum_{(j,k)=(+,-),(-,+)} (\rho_{\rm i})_{jk} \right|\right|_1 = 1 \qquad (10)$$

of coherence. Since modes transform independently under thermal operations, the ω_1 electronic coherence cannot influence the ω_0 populations. If the target *trans* state is an energy eigenstate, therefore, injecting coherence into the electronic state via photoexcitation cannot improve the isomerization yield.

II B. Background: Thermomajorization

The coherences' irrelevance frees us to focus on density matrices' populations when bounding the photoisomerization yield. The thermomajorization preorder governs the populations' evolution under thermal operations [63, 66, 98–104]. Thermomajorization implies necessary and sufficient conditions for the existence of a thermal operation that maps one energy-diagonal state into another.[2]

Thermomajorization can be characterized as follows. Let $H = \sum_{j=1}^{d} E_j |j\rangle\langle j|$ denote a Hamiltonian that governs a state ρ of energy diagonal $\mathcal{D}(\rho) := \sum_j |j\rangle\langle j|\rho|j\rangle\langle j| = \sum_j r_j |j\rangle\langle j|$. Consider rescaling the probabilities with Boltzmann factors, $r_j e^{\beta E_j}$, and ordering the products from greatest to least: $r_{j'} e^{\beta E_{j'}} \geq r_{k'} e^{\beta E_{k'}}$ for all $j' > k'$. Consider the points $\left(\sum_{j'=1}^{\alpha} e^{-\beta E_{j'}}, \sum_{j'=1}^{\alpha} p_{j'}\right)$, for all $\alpha = 1, 2, \ldots, d$. Connecting them with straight lines defines a piecewise-linear curve. This Gibbs-rescaled Lorenz curve is denoted by $L_{(\rho,H)}(x)$, wherein the coordinates run from 0 to the partition function, $Z := \sum_{j=1}^{d} \exp(-\beta E_j)$. Let (σ, H) denote another system, represented by a Lorenz curve $L_{(\sigma,H)}(x)$. If the (ρ, H) curve lies above or on the (σ, H) curve at all x-values, (ρ, H) is said to *thermomajorize* (σ, H). If and only if (ρ, H) thermomajorizes (σ, H) does some thermal operation map the first state's energy diagonal to the second state's:

$$L_{(\rho,H)}(x) \geq L_{(\sigma,H)}(x) \quad \forall x \in [0, Z] \quad \Leftrightarrow \quad \exists \mathcal{T} : \mathcal{T}\big(\mathcal{D}(\rho), H\big) = \big(\mathcal{D}(\sigma), H\big). \qquad (11)$$

Relation (11) generalizes the second law of thermodynamics to arbitrarily small systems and to single-shot transformations. The curve $L_{(\rho,H)}$ illustrates the thermodynamic value of (ρ, H) by codifying the system's informational and energetic resourcefulness.

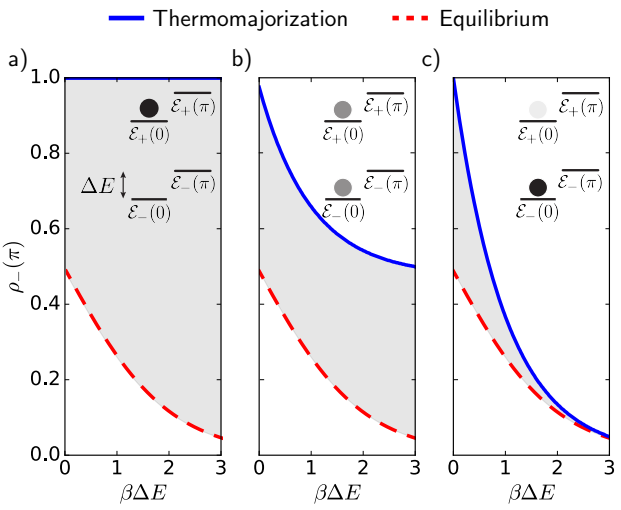

FIG. 2: Thermomajorization bound on the photoisomerization yield $\rho_-(\pi)$ and comparisons with equilibrium statistical mechanics. The red dashed curve shows the predicted equilibrium yield, and the blue solid curve shows the resource-theory bound. Possible optimal yields shown in the gray region from an initially excited state a), from an initial superposition b), and from an unexcited state c). The insets illustrate the molecule's energy levels. The shaded dots show the initial state's probability weights.

II C. Thermomajorization bound on the photoisomerization yield

To bound the optimal photoisomerization yield $\rho_-(\pi)$, we construct the Gibbs-rescaled Lorenz curves for (i) the postexcitation state $\rho_{\rm i} \otimes |\varphi{=}0\rangle\langle\varphi{=}0|$ and (ii) the postrotation state $\rho_{\rm f}$. We then solve for the greatest $\rho_-(\pi)$ that enables the photoexcited state to thermomajorize $\rho_{\rm f}$. The calculations were numerical; the code used is available at dlimmer/QT-PhotoIsomer.

The study has the following focus. We concentrate on the angles $\varphi = 0, \pi$ that define the *cis* and *trans* configurations. Extensions of this four-level model are straightforward and follow from our results, as discussed below. We assess how the bound depends on the *cis-trans* energy gap $\Delta E := \mathcal{E}_-(\pi) - \mathcal{E}_-(0)$, expressed in units of $1/\beta$. We focus on the physically relevant regime in which the

[2] If the states are not energy-diagonal, a generalization of thermomajorization encapsulates the necessary and sufficient conditions [106]. Bounding photoisomerization does not require the generalization: The coherences cannot affect the photoisomerization yield, which is one of the populations (Sec. II A).

ground-state-to-metastable-state gap is far less than the *cis* gap: $\Delta E \ll \mathcal{E}_+(0) - \mathcal{E}_-(0) =: E_1$.

Figure 2 shows results for three photoexcited states $\rho_{\rm i}$. These states interpolate between two extremes, the fully excited $|\psi_1\rangle|\varphi{=}0\rangle$ and the ground state $|\psi_0\rangle|\varphi{=}0\rangle$. If the laser fails to excite the molecule, thermal excitations drive any isomerization. In all three cases, we can identify kinetic setups in which the photoisomerization yield saturates the resource-theory bound (App. B 1).

We compare the resource-theory bound with the Boltzmann-factor yield predicted by equilibrium statistical mechanics, $\rho_-(\pi) = \exp[-\beta\mathcal{E}_-(\pi)]/Z_{\rm mol}$. For all $\rho_{\rm i}$, the equilibrium yield lies below the thermomajorization bound, as required. Moreover, the equilibrium yield lower-bounds the optimal yield: Any additional kinetic preference for converting *cis* to *trans* increases the yield. With thermomajorization upper-bounding possible outcomes, and equilibrium statistical mechanics lower-bounding them, we obtain a range of possible yields as a function of $\rho_{\rm i}$ and ΔE.

Suppose that the laser fully excites the molecule, to $\rho_{\rm i} = |\mathcal{E}_+(0)\rangle\langle\mathcal{E}_+(0)|$. Thermomajorization caps the yield trivially at one, as shown in Fig. 2a). Hence energy conservation and the fixed-temperature bath do not limit the isomerization yield. The unboundedness persists across the physically reasonable gaps $\Delta E \ll E_1$.

If the laser half-excites the molecule, such that $\mathcal{D}(\rho_{\rm i}) = \frac{1}{2}|\mathcal{E}_+(0)\rangle\langle\mathcal{E}_+(0)| + \frac{1}{2}|\mathcal{E}_-(0)\rangle\langle\mathcal{E}_-(0)|$, the yield obeys the bounds in Fig. 2b). When $\Delta E = 0$, the thermomajorization bound < 1. As ΔE grows, the bound approaches 1/2. The bound remains 1/2 for greater values of ΔE than the plot shows.

If the laser fails to excite the molecule significantly, $\rho_{\rm i} = (1-\epsilon)|\mathcal{E}_-(0)\rangle\langle\mathcal{E}_-(0)| + \epsilon|\mathcal{E}_+(0)\rangle\langle\mathcal{E}_+(0)|$, wherein $\epsilon \ll 1$. Thermal excitations drive the isomerization, whose bounds are shown in Fig. 2c). At large ΔE, the resource-theory bound asymptotes to ϵ. The bound approaches 1 as ΔE shrinks to 0.

Resource-theory insights explain several trends. If the laser fully excites the molecule, we saw, thermomajorization implies only that $\rho_-(\pi) \leq 1$. The reason follows from how, as reflected in $L_{(\rho,H)}$, thermodynamic resourcefulness decomposes into information and energy. The initial state is an energy eigenstate, $\rho_{\rm i} = |\mathcal{E}_+(0)\rangle\langle\mathcal{E}_+(0)|$, so an energy measurement's outcome is perfectly predictable. $\rho_{\rm i}$ therefore encodes maximal information. $\rho_{\rm i}$ also has more energetic value than the lower *trans* state, as $E_1 > \Delta E$. Hence $\rho_{\rm i}$ has far more resourcefulness than $|\mathcal{E}_-(\pi)\rangle$. The fundamental thermodynamic limitations of energy conservation and temperature do not constrain the ability of $\rho_{\rm i}$ to transform into $|\mathcal{E}_-(\pi)\rangle$. Only kinetic practicalities, such as relaxation rates, do.

As probability weight shifts downward in $\rho_{\rm i}$, $\rho_{\rm i}$ loses energetic value. $\rho_{\rm i}$ loses also informational value: The diagonal, $\mathcal{D}(\rho_{\rm i})$, grows more mixed. Hence the solid blue curve in Fig. 2b) lies below the solid blue curve in Fig. 2a). But the mixed $\mathcal{D}(\rho_{\rm i})$ retains significant energetic value, since $E_1 \gg \Delta E$. If the laser fails to excite the molecule, $\rho_{\rm i}$ regains informational value, being the energy eigenstate $|\mathcal{E}_-(0)\rangle\langle\mathcal{E}_-(0)|$. The dearth of energy outweighs this informational value, however.

Our four-level model can be extended: The isomer can begin or end in a probabilistic combination of configurations φ. The Gibbs-rescaled Lorenz curves will be calculated by the same procedure. The more the state's weight is distributed across configurations, the less predictable an energy measurement, and so the lesser the state's thermodynamic value. Hence a distribution over initial configurations will lower the bound, and a distribution over final configurations will tighten the bound. Realistic mixtures of final states will be dominated by the $|\varphi{=}0\rangle$ and $|\varphi{=}\pi\rangle$ on which we focus.

II D. Kinetic factors that saturate bound

Can the upper bounds be saturated? We gain insight from a minimal kinetic model of the post-photoexcitation relaxation. We model the molecule's evolution with the Lindblad master equation $\dot{\rho}(t) = -\frac{i}{\hbar}[H, \rho(t)] + \mathcal{L}\big(\rho(t)\big)$. The first term represents the system's coherent dynamics. We again focus on two angular states, so that the minimal Hamiltonian is $H \approx \sum_{\varphi=0,\pi} H_{\rm elec}(\varphi)$ [Eq. (5)]. We set $\mathcal{E}_-(0) = 0$ and, as before, $\mathcal{E}_+(0) = E_1$ and $\mathcal{E}_-(\pi) = \Delta E$. For simplicity, we take $\mathcal{E}_+(\pi) = E_1 + \Delta E$, and we work in the physically relevant regime $E_1 \gg \Delta E > 0$. The levels' populations are denoted by $p_\mu(\varphi)$. The Lindblad equation's second term,

$$\mathcal{L}(\rho) = \sum_i \Gamma_i \left(B_i \rho B_i^\dagger - \frac{1}{2}\{B_i^\dagger B_i, \rho(t)\} \right), \qquad (12)$$

reflects the influence of the bath, which decoheres the state and dissipates energy. We choose Lindblad operators $B_{\mathcal{E}_\mu(\varphi),\mathcal{E}_{\mu'}(\varphi')} = |\mathcal{E}_\mu(\varphi)\rangle\langle\mathcal{E}_{\mu'}(\varphi')|$, for each pair of energy eigenstates. Each B_i dissipates at a rate Γ_i that satisfies local detailed balance, so the system relaxes toward a thermal state. The parameters strongly kinetically prefer relaxation into the *trans* state (App. B 1).

Figure 3 shows the time-dependent densities following relaxation from the initial conditions in Sec. II C. Figure 3a) follows from the fully excited initial state $\rho_{\rm i} = |\mathcal{E}_+(0)\rangle\langle\mathcal{E}_+(0)|$, and Fig. 3 follows from the partially excited $\rho_{\rm i} = \frac{1}{2}|\mathcal{E}_+(0)\rangle\langle\mathcal{E}_+(0)| + \frac{1}{2}|\mathcal{E}_-(0)\rangle\langle\mathcal{E}_-(0)|$. In these cases, the thermomajorization bound is saturated at intermediate times, before thermalization reduces the yield to its equilibrium value. In contrast, Fig. 3c) follows from a barely excited initial state, $\rho_{\rm i} = (1-\epsilon)|\mathcal{E}_-(0)\rangle\langle\mathcal{E}_-(0)| + \epsilon|\mathcal{E}_+(0)\rangle\langle\mathcal{E}_+(0)|$, wherein $\epsilon \ll 1$. The yield maximizes, reaching the resource-theory bound, at very long times set by the large barrier in the ground electronic state, $\mathcal{E}_-(\varphi)$ (Fig. 1).

III. LIMITATIONS ON COHERENCE FOLLOWING PHOTOISOMERIZATION

Photoexcitation may inject coherence into the molecule's state. By "coherence," we mean, coherence relative to the energy eigenbasis in the electronic state. Such coherence might be expected, *a priori*, to contribute to the molecule's rotation. Using the resource-theory tool of monotones, we bound the amount of coherence in $\rho_{\rm f}$. Our argument involves sequential thermal operations, which model, in the resource theory, interactions with a Markovian bath. Markovianity is a common assumption that models rhodopsin's photoisomerization [105]. This coherence has an application detailed in App. B 4: Work can be extracted from the coherence, if photoisomers interact.

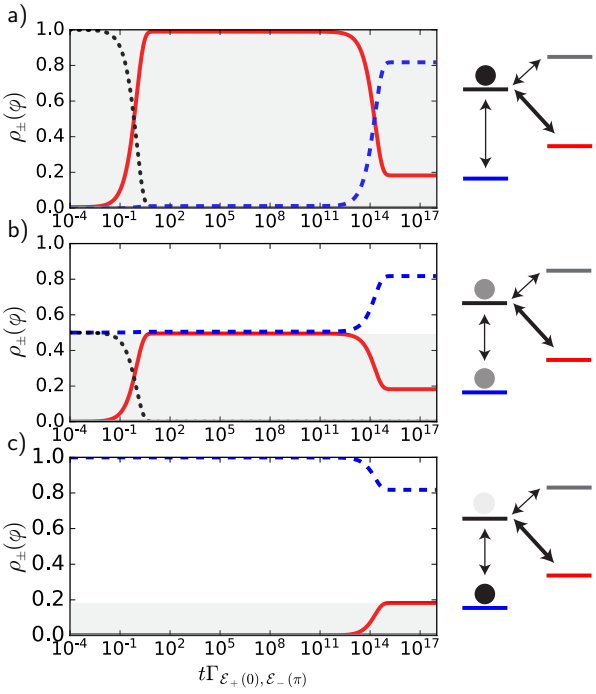

FIG. 3: Comparison of thermomajorization bound with time-dependent Lindblad dynamics. Calculations are performed on the four-level system shown on the right. The filled circles illustrate the initial probability weights, and the arrows signify the possible transitions. Each energy level's population evolves as the correspondingly colored curves in the plots: $|\mathcal{E}_+(0)\rangle$ (dotted black), $|\mathcal{E}_-(\pi)\rangle$ (solid red), $|\mathcal{E}_-(0)\rangle$ (dashed blue), and $|\mathcal{E}_+(\pi)\rangle$ (solid gray). The grayed area denotes the region accessible to $|\mathcal{E}_-(\pi)\rangle$ according to thermomajorization. Population dynamics are shown following a) full excitation to $|\mathcal{E}_+(0)\rangle$, b) half-excitation to a state of energy diagonal $\frac{1}{2}|\mathcal{E}_+(0)\rangle\langle\mathcal{E}_+(0)| + |\mathcal{E}_-(0)\rangle\langle\mathcal{E}_-(0)|$, and c) failure to excite the state significantly: $\rho_{\rm i} = (1-\epsilon)|\mathcal{E}_-(0)\rangle\langle\mathcal{E}_-(0)| + \epsilon|\mathcal{E}_+(0)\rangle\langle\mathcal{E}_+(0)|$, wherein $\epsilon \ll 1$. The parameters used are $\beta\Delta E = 1.5$, $\beta E_1 = 30$, $\beta\hbar\Gamma_{\mathcal{E}_+(0),\mathcal{E}_-(\pi)} = 1$, and $\beta\hbar\Gamma_{\mathcal{E}_+(0),\mathcal{E}_-(0)} = \beta\hbar\Gamma_{\mathcal{E}_+(\pi),\mathcal{E}_+(0)} = 0.01$.

III A. Fisher-information monotone

Focusing on $\varphi = 0, \pi$, we upper-bounded the isomerization yield $\rho_-(\pi)$ (Sec. II C). But we might wish to calculate $\rho_-(\pi)$, using resource-theory tools. We must model the full rotation, $\varphi \in [0, \pi]$, within the resource theory. We do so in App. B 2, treating φ as a quantum clock [71–80]. The chemical groups' angular momentum, ℓ_φ, governs the rotation speed. To illustrate how the momentum can affect the dynamics, we linearize $H_{\rm elec}(\varphi)$ [Eq. (3)] near the avoiding crossing point. For simplicity, we assume that the momentum remains constant.

The resulting Hamiltonian has the form of a Landau-Zener model,

$$H_{\rm LZ}(t) \approx -vt\left(|\psi_1\rangle\langle\psi_1| - |\psi_0\rangle\langle\psi_0|\right) + \frac{\lambda}{2}\left(|\psi_0\rangle\langle\psi_1| + {\rm h.c.}\right) \tag{13}$$

illustrated near the crossing point in Fig. 1. The Hamiltonian changes at a speed $v \propto |d\varphi/dt|$ that has dimensions of energy/time. The time, t, runs from $-\infty$ to ∞ in the Landau-Zener model.

We can understand the model by evaluating limits in an example. Suppose that the molecule begins in the upper diabatic level, $|\psi_1\rangle$. If $v \ll \lambda^2/\hbar$, the state evolves adiabatically, changing from $|\psi_1\rangle$ but remaining in the upper instantaneous eigenstate. If $v \gg \lambda^2/\hbar$, the state evolves diabatically, remaining (approximately) $|\psi_1\rangle$, which becomes approximately the lower energy eigenstate. Isomerization in the presence of a thermal bath amounts to a dissipative Landau-Zener transition [107–110]. We model such transitions within the resource theory in App. III B. Here, we quantify the postisomerization coherence in the electronic state with the quantum Fisher information $I_{\rm F}$ relative to the Hamiltonian, a resource-theory monotone [111].

$I_{\rm F}$ quantifies mixed and pure states' coherences [111, 112].[3] Let ρ denote a quantum state that eigendecomposes as $\rho = \sum_j r_j |j\rangle\langle j|$. The Fisher information with respect to a Hamiltonian H is

$$I_{\rm F}(\rho, H) = 2\sum_{j,k} \frac{(r_j - r_k)^2}{r_j + r_k} \left|\langle j|H|k\rangle\right|^2 . \tag{14}$$

$I_{\rm F}$ quantifies the state's ability to distinguish instants as a quantum clock [111]. When evaluated on a pure state, $I_{\rm F}$ reduces to four times the energy variance, $\langle H^2\rangle - \langle H\rangle^2$.

We can calculate explicitly the Fisher information in the post-photoisomerization state. We temporarily assume that the molecule ends in the *trans* configuration

[3] $I_{\rm F}$ is one of multiple monotones that quantify coherence. Photoisomers' coherence has been measured, for example, with rate-constant behavior [113].

(with $\varphi = \pi$), rather than in a statistical mixture of *cis* and *trans* states. This assumption simplifies the calculation, which can be generalized, and is physically realistic. We eigendecompose the post-photoisomerization state as $\rho_{\rm f} = \rho_{\rm f}^{\rm elec} \otimes |\varphi{=}\pi\rangle\langle\varphi{=}\pi| = \sum_{i,j=0,1} \rho_{ij} |\psi_i\rangle\langle\psi_j| \otimes |\varphi{=}\pi\rangle\langle\varphi{=}\pi|$. For the Landau-Zener Hamiltonian,

$$I_{\rm F}(\rho_{\rm f}^{\rm elec}, H_{\rm LZ}(t_{\rm f})) = \lambda^2 \left| 1 - 2\rho_{00} - 4\,\frac{v t_{\rm f}}{\lambda}\,{\rm Re}(\rho_{01}) \right|^2 , \tag{15}$$

wherein the density matrix and the Hamiltonian are evaluated at $t = t_{\rm f} \gg \lambda/v$. The gap, λ, sets the distance tuned through in energy space, due to (i) the Hamiltonian's linearization and (ii) the order-one change in the angle, π. We have invoked the state's normalization, $\rho_{00} + \rho_{11} = 1$. We simplify and bound Eq. (15) in App. B 3. The result is

$$\begin{aligned} &I_{\rm F}(\rho_{\rm f}^{\rm elec}, H_{\rm LZ}(t_{\rm f})) \\ &\leq I_{\rm F}^{+} := 16 v^2 t_{\rm f}^2 e^{-\pi\lambda^2/(2\hbar v)} \left(1 - e^{-\pi\lambda^2/(2\hbar v)}\right) . \end{aligned} \tag{16}$$

The proportionality to the squared momentum, $(v t_{\rm f})^2$, quantifies how underdamping near the avoided crossing generates more coherence than overdamping would generate. An expression similar to Eq. 16 has been derived in the context of parameter estimation on a closed Landau-Zener transition [114].

III B. Dissipative Landau-Zener transition

To study the bath's effects on the Landau-Zener evolution of the electronic coherences, we have evaluated $I_{\rm F}$ on the molecule's postrotation state, $\rho_{\rm f}$, again using the Lindblad master equation. The system Hamiltonian H approximately has the Landau-Zener form $H_{\rm LZ}(t)$. We suppose that the system couples to the bath through the operator $B = |\psi_1\rangle\langle\psi_1| - |\psi_0\rangle\langle\psi_0|$. Relative to the $H_{\rm LZ}(t)$ eigenbasis near the avoided crossing, B is represented by a nondiagonal matrix. Hence B transfers population between energy levels, at a rate Γ. At frequencies resonant with the photoisomer away from the avoided crossing, the bath's density of states is expected to be vanishingly small. Thus, away from the avoided crossing, the bath's action can be ignored to first order in the system-bath coupling. This Lindbladian and alternatives have been ascribed to the Landau-Zener transition elsewhere [109].

To obtain $\rho_{\rm f}$, we prepared the electronic state $|\psi_1\rangle$ and simulated evolution from times $t = -t_{\rm f}$ to $t_{\rm f} = 50\hbar/\lambda$. For simplicity, we adopt a unit system in which $\lambda = \hbar = 1$. We focus on the dependences on v and Γ.

Figure 4a) shows the photoisomerization yields, under Landau-Zener dynamics, for different decohence rates. If $\Gamma = 0$, the yield is well-described by the canonical Landau-Zener transition probability $\rho_-(\pi) = \rho_{11} \approx \exp\left(-\frac{\pi\lambda^2}{2\hbar v}\right)$. At low speeds, $v\hbar/\lambda^2 \ll 1$, the yield is small. The system evolves adiabatically, ending in the diabatic state $|\psi_0\rangle$. At high speeds, $v\hbar/\lambda^2 \gg 1$, the yield is greater: The system lacks time to transition to $|\psi_0\rangle$ and so remains in $|\psi_1\rangle$.

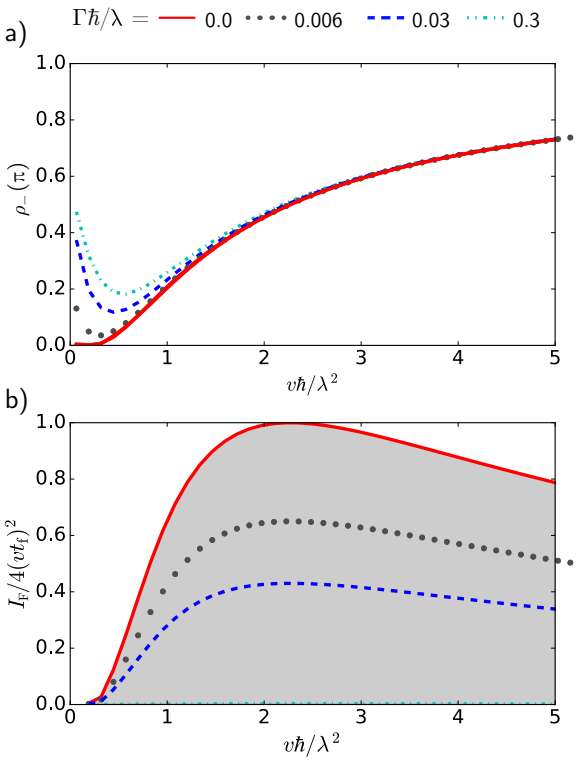

FIG. 4: Dissipative Landau-Zener model for the lower *trans* state's population and for coherence, relative to the energy eigenbasis, in the electronic state. The initial state, $|\psi_1\rangle$, was evolved from an initial time of $-t_{\rm f}$ to $t_{\rm f} = 50\,\hbar/\lambda$. a) Final lower-*trans*-level population as a function of transition speed, v, for different dephasing rates Γ. b) Reduced Fisher information, as a function of v for different dephasing rates Γ. The grayed area represents the monotone bound (16).

Consider raising the phase-damping rate Γ at a fixed v. If the speed is low, $v\hbar/\lambda^2 \ll 1$, the yield rises. If the speed is large, $v/\lambda \gg \Gamma$, the yield about equals its decoherence-free value, regardless of Γ. The yield minimizes when $\Gamma \approx v/\lambda$: The decoherence's mixing of energy eigenstates, which transfers about half the state's weight to the lower energy level, balances adiabaticity's preservation of the upper level's weight.

Similar behavior was observed in [109]. See [115, 116] for further treatments of coherence in dissipative Landau-Zener transitions. Whereas earlier work focused mostly on the populations, we quantify how the electronic energy coherences evolve in the dissipative Landau-Zener problem.

Figure 4b) shows the Fisher information scaled by

$1/(4v^2t_{\rm f}^2)$. When $\Gamma = 0$, $I_{\rm F}$ adheres to the asymptotic prediction $I_{\rm F}^+$ [Eq. (16)], represented by the grayed region. The asymptotic bound (16) limits the coherence, we verified, for finite Γ. Raising Γ above 0 decreases the scaled Fisher information toward 0.

The scaled coherence peaks at an intermediate speed given by Eq. (16). At this v, half the population transitions from the initial excited state, $|\psi_1\rangle$, to the final ground state, $|\psi_1\rangle$. Transitioning half the population spreads probability weight evenly across the energy levels. Even spreading accompanies maximal coherence. This observation agrees with the quantum adiabatic theorem: If $H_{\rm LZ}(t)$ changes slowly, the electronic DOF remains in an instantaneous energy eigenstate. The final state, $|\mathcal{E}_+(\pi)\rangle$, therefore lacks coherence. If $H_{\rm LZ}(t)$ changes quickly, the state has no time evolve away from $|\psi_1\rangle$. Since $|\psi_1\rangle$ becomes the $H_{\rm LZ}(t_{\rm f})$ ground level, the final state again lacks coherence. Hence low and high v's lead to small coherences that we have quantified with $I_{\rm F}/(4v^2t_{\rm f}^2)$.

In summary, isomerization partially trades off with electronic coherences relative to the energy eigenbasis. Little population transfer, which is undesirable, accompanies little coherence. Little coherence accompanies also a desirable large population transfer. Midsize population transfer accompanies large coherences. We have quantified these trends with the Fisher information. Moreover, electronic energy coherences do not straightforwardly promote isomerization in this minimal model.

IV. DISCUSSION

We have derived fundamental limitations on photoisomerization, using thermodynamic resource theories. The bounds are simple, general, and derived from few assumptions. Yet the results shed light on the roles played by information, energy, and coherence in molecules prevalent in natural and artificial materials.

Similar insights may follow from modeling other chemical systems with thermodynamic resource theories. Candidates include chlorophyll [117–120] and photovoltaics [121–125]. Exciton transport there may be bounded as isomerization is here. Additionally, azobenzene has been attached to carbon nanotubes [31]. The attachment raised the isomers' capacity for storing solar fuel by 200%, though 30% was expected. The improvements achievable—and the engineering effort exerted—might be upper-bounded with a variation on our model.

This work leverages resource theories, which have remained largely abstract, to solve known problems in experimental systems. A bridge for thermodynamic resource theories from mathematical physics to the real physical world was called for recently [126]; construction has just begun [91, 127–129]. Experimental proposals designed to realize resource-theory results have provided a valuable first step. The present paper progresses from artifice to explaining diverse phenomena realized already in nature and in experiments, to answering questions already asked in atomic, molecular, and optical physics and chemistry. This program may be advanced through this paper's resource-theory model for Landau-Zener transitions, which occur across chemistry and many-body physics.

ACKNOWLEDGMENTS

NYH thanks Bassam Helou, David Jennings, Christopher Perry, and Mischa Woods for conversations. NYH is grateful for funding from the Institute for Quantum Information and Matter, an NSF Physics Frontiers Center (NSF Grant PHY-1125565) with support from the Gordon and Betty Moore Foundation (GBMF-2644), for a Barbara Groce Graduate Fellowship, for a KITP Graduate Fellowship (the KITP receives support from the NSF under Grant No. NSF PHY-1125915), and for an NSF grant for the Institute for Theoretical Atomic, Molecular, and Optical Physics at Harvard University and the Smithsonian Astrophysical Observatory. DTL was supported by UC Berkeley College of Chemistry and by the Kavli Energy NanoSciences Institute.

Appendix A EVERY COMPOSITION OF THERMAL OPERATIONS IS A THERMAL OPERATION.

Let (ρ, H) represent a system $\mathcal{S}$ of interest. $\mathcal{S}$ evolves under an arbitrary thermal operation $\mathcal{E}$ as

$$(\rho, H) \mapsto \mathcal{E}(\rho, H) = \left({\rm Tr}_{\rm a} \left(U \left[\rho \otimes e^{-\beta H_{\mathcal{B}}}/Z \right] U^\dagger \right), H + H_{\mathcal{B}} - H_{\rm a} \right). \tag{A1}$$

$H_{\mathcal{B}}$ denotes the bath Hamiltonian, and $Z := {\rm Tr}\left(e^{-\beta H_{\mathcal{B}}}/Z \right)$ denotes the partition function. a denotes a discarded ancilla that is not coupled to the rest of the system by any term in $H + H_{\mathcal{B}}$. The unitary U preserves the total Hamiltonian: $[U, H + H_{\mathcal{B}}] = 0$. Let $\tilde{\mathcal{E}}$ denote another thermal operation:

$$(\rho, H) \mapsto \tilde{\mathcal{E}}(\rho, H) = \left({\rm Tr}_{\tilde{\rm a}} \left(\tilde{U} \left[\rho \otimes e^{-\beta H_{\tilde{\mathcal{B}}}}/\tilde{Z} \right] \tilde{U}^\dagger \right), H + H_{\tilde{\mathcal{B}}} - H_{\tilde{\rm a}} \right). \tag{A2}$$

The tilded quantities are defined analogously to their tilde-free analogues. Consider composing the thermal operations:

$$(\rho, H) \mapsto \tilde{\mathcal{E}}(\mathcal{E}(\rho, H)) \tag{A3}$$

$$= \Bigg(\mathrm{Tr}_{\tilde{\mathrm{a}}} \left(\tilde{U} \left\{ \mathrm{Tr}_{\mathrm{a}} \left(U \left[\rho \otimes e^{-\beta H_{\mathcal{B}}}/Z \right] U^\dagger \right) \otimes e^{-\beta H_{\tilde{\mathcal{B}}}}/\tilde{Z} \right\} \tilde{U}^\dagger \right), \tag{A4}$$

$$H + H_{\mathcal{B}} - H_{\mathrm{a}} + H_{\tilde{\mathcal{B}}} - H_{\tilde{\mathrm{a}}} \Bigg).$$

We will show that the composite is a thermal operation:

$$\tilde{\mathcal{E}}(\mathcal{E}(\rho, H)) = \left(\mathrm{Tr}_{\bar{\mathrm{a}}} \left(\bar{U} \left[\rho \otimes e^{-\beta H_{\bar{\mathcal{B}}}}/\bar{Z} \right] \bar{U}^\dagger \right), H + H_{\bar{\mathcal{B}}} - H_{\bar{\mathrm{a}}} \right), \tag{A5}$$

for some bath Hamiltonian $\bar{\mathcal{B}}$, some unitary $\bar{U}$, and some uncoupled ancilla $\bar{\mathrm{a}}$.

Let us return to Eq. (A4). The tensoring on of $e^{-\beta H_{\tilde{\mathcal{B}}}}/\tilde{Z}$ does not change the state of a. Nor does $\tilde{U}$ act on the Hilbert space of a. Hence the tensoring on and the $\tilde{U}$ commute with the $\mathrm{Tr}_{\mathrm{a}}(.)$. During the commutation, an $\mathbb{1}_{\mathcal{B}}$ is tensored onto the $\tilde{U}$, such that $\tilde{U} \otimes \mathbb{1}_{\mathcal{B}}$ acts on the Hilbert space of $\mathcal{S} + \mathcal{B} + \tilde{\mathcal{B}}$. The traces compose as $\mathrm{Tr}_{\tilde{\mathrm{a}}}(\mathrm{Tr}_{\mathrm{a}}(.)) = \mathrm{Tr}_{\tilde{\mathrm{a}}+\mathrm{a}}(.) \equiv \mathrm{Tr}_{\bar{\mathrm{a}}}(.)$:

$$\tilde{\mathcal{E}}(\mathcal{E}(\rho, H)) = \Bigg(\mathrm{Tr}_{\bar{\mathrm{a}}} \left(\left[\tilde{U} \otimes \mathbb{1}_{\mathcal{B}} \right] \left\{ U \left[\rho \otimes e^{-\beta H_{\mathcal{B}}}/Z \right] U^\dagger \otimes e^{-\beta H_{\tilde{\mathcal{B}}}}/\tilde{Z} \right\} \left[\tilde{U} \otimes \mathbb{1}_{\mathcal{B}} \right]^\dagger \right),$$

$$H + H_{\mathcal{B}} + H_{\tilde{\mathcal{B}}} - H_{\bar{\mathrm{a}}} \Bigg). \tag{A6}$$

The U does not act on the $\tilde{\mathcal{B}}$ Hilbert space. Hence the U commutes with the tensoring on of $e^{-\beta H_{\tilde{\mathcal{B}}}}/\tilde{Z}$. In commuting the U out, we must tensor onto it a $\mathbb{1}_{\tilde{\mathcal{B}}}$. The unitaries compose as $(\tilde{U} \otimes \mathbb{1}_{\mathcal{B}})(U \otimes \mathbb{1}_{\tilde{\mathcal{B}}}) =: \bar{U}$. This operator is unitary and conserves the global Hamiltonian, $H + H_{\mathcal{B}} + H_{\tilde{\mathcal{B}}}$. Hence

$$\tilde{\mathcal{E}}(\mathcal{E}(\rho, H)) = \left(\mathrm{Tr}_{\bar{\mathcal{B}}} \left(\bar{U} \left[\rho \otimes e^{-\beta H_{\mathcal{B}}}/Z \otimes e^{-\beta H_{\tilde{\mathcal{B}}}}/\tilde{Z} \right] \bar{U}^\dagger \right), H + H_{\mathcal{B}} + H_{\tilde{\mathcal{B}}} - H_{\bar{\mathrm{a}}} \right). \tag{A7}$$

The composition of two Gibbs states is a Gibbs state: $e^{-\beta H_{\mathcal{B}}}/Z \otimes e^{-\beta H_{\tilde{\mathcal{B}}}}/\tilde{Z} = e^{-\beta H_{\bar{\mathcal{B}}}}/\bar{Z}$, wherein $H_{\bar{\mathcal{B}}} := H_{\mathcal{B}} + H_{\tilde{\mathcal{B}}}$. Equation (S5) therefore has the form of Eq. (S7).

Appendix B WHY MODES OF COHERENCE TRANSFORM INDEPENDENTLY UNDER THERMAL OPERATIONS

This note reviews why modes of coherence transform independently under thermal operations. The independence rests on thermal operations' covariance with respect to the time translations generated by the system-of-interest Hamiltonian. The note relies on [97], by Marvian and Spekkens, and on [70], by Lostaglio *et al.* Marvian and Spekkens reason generally about U(1) symmetry. Lostaglio *et al.* tailor Marvian and Spekkens's results to time-translation symmetry, basing their conclusions on Marvian and Spekkens's arguments.

System of interest, decompositions, and definitions: Let $\mathcal{S} = (\rho, H)$ denote the initial system. The operators are defined on a Hilbert space $\mathcal{H}$. Lostaglio *et al.* focus on nondegenerate Hamiltonians H. (The molecule's Hamiltonian lacks degeneracies in our study.) The Hamiltonian eigendecomposes as $H|n\rangle = \omega_n|n\rangle$.

We can decompose the state in terms of the energy eigenbasis: $\rho = \sum_{n,m} \rho_{nm}|n\rangle\langle m|$. The coefficients ρ_{nm} form a matrix. Column n corresponds to the energy ω_n, and row m corresponds to the energy ω_m. The gap $\omega_n - \omega_m$ defines a mode. Multiple elements ρ_{nm} can correspond to the same mode. Summing these elements yields "the component of ρ in mode ω":

$$\rho^{(\omega)} := \sum_{n,m\,:\,\omega_n - \omega_m = \omega} \rho_{nm}|n\rangle\langle m|. \tag{B1}$$

The state decomposes in terms of modes as

$$\rho = \sum_{\omega} \rho^{(\omega)}. \tag{B2}$$

Consider evolving a $\rho^{(\omega)}$ under the system's Hamiltonian. The mode acquires a phase:

$$\rho^{(\omega)} = e^{-iHt}\rho^{(\omega)}e^{iHt} = e^{-i\omega t}\rho^{(\omega)}. \tag{B3}$$

Thermal operations: Let $\mathcal{E}$ denote any thermal operation in which the bath, and only the bath, is discarded:

$$\mathcal{E}((\rho, H)) = (\sigma, H), \tag{B4}$$

for some density operator σ defined on $\mathcal{H}$. The thermal operation is covariant with respect to the translations generated by H: Let $H_{\mathcal{B}}$ denote the Hamiltonian of the bath system that couples to $\mathcal{S}$, $\mathcal{B} = (e^{-\beta H_{\mathcal{B}}}/Z, H_{\mathcal{B}})$. For every operator O defined on $\mathcal{H}$,

$$\mathcal{E}\left(e^{-iHt}Oe^{iHt}\right) = \mathrm{Tr}_{\mathcal{B}}\left(U\left[e^{-iHt}Oe^{iHt}\otimes e^{-\beta H_{\mathcal{B}}}/Z\right]U^{\dagger}\right) \tag{B5}$$

$$= \mathrm{Tr}_{\mathcal{B}}\left(U\left[e^{-iHt}Oe^{iHt}\otimes e^{-iH_{\mathcal{B}}t}(e^{-\beta H_{\mathcal{B}}}/Z)e^{iH_{\mathcal{B}}t}\right]U^{\dagger}\right) \tag{B6}$$

$$= \mathrm{Tr}_{\mathcal{B}}\left(U\left\{e^{-i(H+H_{\mathcal{B}})t}\left[O\otimes e^{-\beta H_{\mathcal{B}}}/Z\right]e^{i(H+H_{\mathcal{B}})t}\right\}\right) \tag{B7}$$

$$= \mathrm{Tr}_{\mathcal{B}}\left(e^{-i(H+H_{\mathcal{B}})t}U\left[O\otimes e^{-\beta H_{\mathcal{B}}}/Z\right]U^{\dagger}e^{i(H+H_{\mathcal{B}})t}\right) \tag{B8}$$

$$= e^{-iHt}\mathrm{Tr}_{\mathcal{B}}\left(U\left[O\otimes e^{-\beta H_{\mathcal{B}}}/Z\right]U^{\dagger}\right)e^{iHt} \tag{B9}$$

$$= e^{-iHt}\mathcal{E}(O)e^{iHt}. \tag{B10}$$

The first equality follows from the thermal operation's definition. Equation (B6) follows from the bath state's invariance under the time translations generated by $H_{\mathcal{B}}$. Equation (B7) follows from the commutation of H with $H_{\mathcal{B}}$. The commutation of U with $H + H_{\mathcal{B}}$, codified in the definition of $\mathcal{E}$, implies Eq. (B8). Equation (B9) represents the equivalence of two protocols: (i) evolving the whole system under $H + H_{\mathcal{B}}$, then discarding the bath, and (ii) discarding the bath, then evolving $\mathcal{S}$ under H.

Claim: Let

$$\sigma = \sum_{\omega}\sigma^{(\omega)} \tag{B11}$$

denote the mode decomposition of σ. We wish to prove that the coherences relative to the H eigenbasis transform independently under the thermal operations in which the bath, and only the bath, is traced out:

$$\mathcal{E}\left(\rho^{(\omega)}\right) = \sigma^{(\omega)}. \tag{B12}$$

We substitute $O = \rho^{\omega}$ into Eq. (B10):

$$e^{-iHt}\mathcal{E}\left(\rho^{(\omega)}\right)e^{iHt} = \mathcal{E}\left(e^{-iHt}\rho^{(\omega)}e^{iHt}\right) \tag{B13}$$

$$= \mathcal{E}\left(e^{-i\omega}\rho^{(\omega)}\right) \tag{B14}$$

$$= e^{-i\omega}\mathcal{E}\left(\rho^{(\omega)}\right). \tag{B15}$$

Equation (B14) follows from Eq. (B3). Equation (B15) follows from the convex linearity of quantum operations, which include thermal operations.[4] The left-hand side of Eq. (B13), with Eq. (B15), implies that $\mathcal{E}\left(\rho^{(\omega)}\right)$ belongs to mode ω. Therefore, by Eq. (B11), $\mathcal{E}\left(\rho^{(\omega)}\right)$ is $\sigma^{(\omega)}$.

B 1 Details about Lindblad evolution

We choose Lindblad operators $B_{\mathcal{E}_\mu(\varphi),\mathcal{E}_{\mu'}(\varphi')} = |\mathcal{E}_\mu(\varphi)\rangle\langle\mathcal{E}_{\mu'}(\varphi')|$, for each pair of energy eigenstates. Each B_i dissipates at a rate Γ_i assumed to satisfy local detailed balance,

$$\frac{\Gamma_{\mathcal{E}_\mu(\varphi),\mathcal{E}_{\mu'}(\varphi')}}{\Gamma_{\mathcal{E}_{\mu'}(\varphi'),\mathcal{E}_\mu(\varphi)}} = e^{-\beta[\mathcal{E}_\mu(\varphi)-\mathcal{E}_{\mu'}(\varphi')]}, \tag{B16}$$

---

[4] Convex-linear operators O map convex combinations to convex combinations: If $\{p_j\}$ denotes a probability distribution and ρ_j denotes a density operator defined on $\mathcal{H}$, $O\left(\sum_j p_j\rho_j\right) = \sum_j p_j O(\rho_j)$.

so the system relaxes toward a thermal state. To model the slowness of thermal isomerization, we set $\Gamma_{\mathcal{E}_-(0),\mathcal{E}_-(\pi)} = \Gamma_{\mathcal{E}_-(\pi),\mathcal{E}_-(0)} = 0$. Also processes involving the high-energy state $|\mathcal{E}_+(\pi)\rangle$ can be ignored. The numerical evaluations of the master equation were accomplished using QuTip code [130].

The Lindblad equation can be solved analytically, though the solution is complicated. We can gain intuition from the regime

$$\Gamma_{\mathcal{E}_+(0),\mathcal{E}_-(\pi)} \gg \Gamma_{\mathcal{E}_+(0),\mathcal{E}_-(0)}, \tag{B17}$$

in which relaxation into the *trans* state is kinetically preferred. Furthermore, satisfying Ineq. (B17) and

$$E_1 \gg \Delta E \tag{B18}$$

simultaneously enables the Lindblad evolution to saturate the resource-theory bounds, as we shall see. Under Ineq. (B17), the ground *trans* state has a population of

$$\rho_-(\pi) = \frac{1}{1 + e^{\beta(\Delta E - E_1)}} \left(1 - e^{-tk}\right) \tag{B19}$$

at early times $t \ll 1/\Gamma_{\mathcal{E}_+(0),\mathcal{E}_-(0)}$. The population grows, from 0 at $t = 0$, with the effective rate $k = \Gamma_{\mathcal{E}_+(0),\mathcal{E}_-(\pi)} + \Gamma_{\mathcal{E}_-(\pi),\mathcal{E}_+(0)}$. Our qualitative results are insensitive to the specific parameters studied, if the constants satisfy Ineqs. (B17) and (B18). In the intermediate-time limit, $1/\Gamma_{\mathcal{E}_+(0),\mathcal{E}_-(0)} \gg t \gg 1/k$, the molecule likely isomerizes: $\rho_-(\pi)$ approaches 1.

B 2 Resource-theory model for dissipative Landau-Zener problem

We model the dissipative Landau-Zener transition of Sec. III B within the thermodynamic resource theory. This quantum-information approach may offer insights into the interplay between energy and coherence in Landau-Zener transitions across chemistry and condensed matter.

Clocks: The Landau-Zener problem involves a speed v and so time. In contrast, every thermal operation $\mathcal{T}$ has time-translation covariance [90]: $e^{-iHt}\mathcal{T}(\rho)e^{iHt} = \mathcal{T}\left(e^{-iHt}\rho e^{iHt}\right)$, if ρ denotes a state governed by the Hamiltonian H. We must therefore introduce a clock into our resource-theory formalism [52, 53, 55, 56, 75–80, 131]. Clocks have been modeled as instances of more-general reference frames [76–80], A reference frame is a resource that effectively lifts a superselection rule such as energy conservation. A good clock occupies an even superposition of many energy eigenstates [52, 53, 55, 56, 75, 131] and so has substantial coherence. A clock can dictate which Hamiltonian governs the system of interest at any given instant.

Molecular clock: The molecular configuration φ serves as a clock in Eq. (3). The rotating chemical group, shown in Fig. 1, serves as the clock hand. When $\varphi = 0$, the hand effectively points to 12:00, and the *cis* Hamiltonian $H_{\rm elec}(\varphi{=}0)$ governs the electronic DOF. When $\varphi = \pi$, the hand effectively points to 6:00, and the *trans* Hamiltonian $H_{\rm elec}(\varphi{=}\pi)$ governs the electronic DOF.

A reliable clock hand has at least two properties: (i) Which number the hand points to can be distinguished. (ii) The clock hand sweeps across the clock face steadily. To serve as a good clock, therefore, the chemical group should have a well-defined angular position φ and a well-defined angular momentum ℓ_φ. The chemical group can have both due to its semiclassicality: Being large, the chemical group collides with other molecules frequently. The collisions localize the chemical group spatially. Being heavy, the chemical group is expected to have a large angular momentum: $\langle \ell_\varphi \rangle \sim \frac{\hbar}{mr}$, wherein m denotes the mode's effective mass and r denotes the molecule's radius. The configuration occupies a state analogous to a coherent state of light [77, 132] and to the Gaussian clock state in [78].

Evolution: As the molecule rotates, the clock hand ticks forward. To simplify the discussion, we will use the Schrödinger picture. In contrast, many thermodynamic-resource-theory calculations are performed in the interaction picture: Consider a system $\mathcal{S}$ that interacts with a bath $\mathcal{B}$ during a thermal operation $\mathcal{T}$. A Hamiltonian-conserving unitary U evolves $\mathcal{S}+\mathcal{B}$: $[U, H_\mathcal{S} + H_\mathcal{B}] = 0$. The conservation enables us to ignore the evolution generated by $H_\mathcal{S} + H_\mathcal{B}$.

We discretize $\varphi \in [0, 2\pi]$ into $2f$ values, for a fixed value of f:

$$H_{\rm mol} = \sum_{j=0}^{2f-1} \left[H_{\rm elec}(\varphi_j) \otimes |\varphi_j\rangle\langle\varphi_j| + \mathbb{1}_{\rm elec} \otimes \frac{\ell_\varphi^2}{2m} \right]. \tag{B20}$$

When $t = 0$, $\varphi_0 = 0$, and when $t = t_f$, $\varphi = \pi$. We extend the angle to be $\varphi \in [0, 2\pi)$, such that $\varphi_{2f} = \varphi_0$. This extension can facilitate the mathematics regardless of whether a photoisomer opens to $\varphi = \pi$ or to $\varphi = 2\pi$. We have discretized φ for physical realism and for convenience of application of resource-theory results. Discretizing φ,

using an analogue of the discrete-variable representation basis [133], is formally equivalent to truncating the energy eigenbasis with a high-energy cutoff. Because we focus on finite-energy excitations, instantaneous energy eigenstate with energies much higher than the initial state's can be ignored: They will not couple to the evolution during the Landau-Zener transition. Resource theorists often prefer to study discrete systems. Yet a continuous version of the Lorenz curve, the cumulous distribution function, exists. Furthermore, a model for extending resource-theory results to continuous appears in App. G of [93].

We model the evolution as a sequence of two alternating time steps: (i) A "tick operation" shifts the clock hand forward, changing the Hamiltonian $H_{\rm elec}(\varphi)$ experienced by the electronic DOF. We model the electronic state as approximately constant during this time step. (ii) The new $H_{\rm elec}(\varphi)$ evolves the electronic state for a time Δt. The greater the Δt, the more slowly the molecule rotates.

Speeds: This model has three regimes: the sudden-quench limit, the quantum-adiabatic limit, and intermediate speeds. Let us introduce these regimes in turn. To facilitate understanding, we suppose that the electronic DOF begins in an eigenstate $|\mathcal{E}_+(0)\rangle$ of $H_{\rm elec}(0)$.

In the sudden-quench limit, $\Delta t \ll \frac{\hbar}{\mathcal{E}_+(\varphi) - \mathcal{E}_-(\varphi)}$ for all φ. No intermediate $H_{\rm elec}(\varphi)$'s have time to evolve the electronic DOF. The electronic state remains $|\mathcal{E}_+(0)\rangle$, while $H_{\rm elec}(\varphi)$ changes drastically. The final electronic state may therefore have coherence relative to the final energy eigenbasis.

In the quantum-adiabatic limit, $\Delta t \gg \frac{\hbar}{\mathcal{E}_+(\varphi) - \mathcal{E}_-(\varphi)}$ for all φ. After the first time step, $H_{\rm elec}(\varphi_1)$ evolves the electronic state $|\mathcal{E}_+(0)\rangle$. A matrix diagonal relative to the $H_{\rm elec}(\varphi_0)$ eigenbasis represents the initial state, $|\mathcal{E}_+(0)\rangle\langle\mathcal{E}_+(0)|$, while an off-diagonal matrix represents $H_{\rm elec}(\varphi_1)$. The off-diagonal elements change the state. The change is sizable, because Δt is large. In the $\Delta t \to \infty$ limit, the change evolves the state into an eigenstate of $H_{\rm elec}(\varphi_1)$.

In the intermediate regime, $\Delta t \approx \frac{\hbar}{\mathcal{E}_+(\varphi) - \mathcal{E}_-(\varphi)}$. Each new $H_{\rm elec}(\varphi)$ updates the state, but not to an eigenstate of the instantaneous Hamiltonian.

Ticking operation: To introduce the ticking operation, we temporarily disregard the bath. The operator

$$U_{\rm tick} := \mathbb{1}_{\rm elec} \otimes \sum_{j=0}^{2f-1} |\varphi_{j+1}\rangle\langle\varphi_j| \tag{B21}$$

rotates the molecule. The operator is unitary, $U_{\rm tick}^\dagger U_{\rm tick} = U_{\rm tick} U_{\rm tick}^\dagger = \mathbb{1}_{\rm elec} \otimes \mathbb{1}_\varphi$, by the modularity of φ.

The system-and-clock Hamiltonian can generate $U_{\rm tick}$ if the clock evolves under a Hamiltonian proportional to its momentum [71–74, 76, 78]. This requirement stipulates, in our case, that $H_\varphi = c\ell_\varphi$. The constant $c \in \mathbb{R}$ can be set to one. This Hamiltonian has an eigenspectrum unbounded from below and so is unphysical. If the clock Hamiltonian were physical, we could use this result to model, resource-theoretically, a molecule tumbling by itself.

Nevertheless, we can use the ideal clock to understand how the molecule's angular DOF serves as an imperfect clock. The ideal clock's $H_\varphi \propto \ell_\varphi$ kicks the clock hand forward: H_φ generates a unitary $e^{-\frac{i}{\hbar}\ell_\varphi t}$ that evolves the clock as $|\varphi_j\rangle \mapsto e^{-\frac{i}{\hbar}\ell_\varphi t}|\varphi_j\rangle = |\varphi_j + t\rangle \equiv |\varphi_{j+1}\rangle$. Again, we have translated the notation of [76] into our notation.

Our clock's Hamiltonian equals the kinetic energy T in Eq. (3): $H_\varphi = \frac{(\ell_\varphi)^2}{2mr^2}$. This H_φ not only shifts the angular DOF forward, but also spreads out the DOF's state in position space. This spreading is not expected to change the state much, due to the chemical group's near-classicality. To reconcile the molecule's Hamiltonian with the quantum-clock formalism more precisely, one might adapt [78]. In [78], Woods *et al.* approximate the $H_c \propto \ell_\varphi$ clock with an oscillator whose Hilbert space has a finite dimensionality.

Dissipative ticking operation: Let us reincorporate the bath into the model. While rotating, the molecule jostles bath particles. They carry off energy dissipated as $H_{\rm elec}(\varphi)$ changes.

To model the dissipation, we assume that the bath Hamiltonian's spectrum is dense and contains gaps of all sizes: For every electronic energy eigenstate $|\mathcal{E}_\pm(\varphi_j)\rangle$, $H_\mathcal{B}$ has eigenstates $|\mathscr{E}_j^\pm\rangle$ and $|\mathscr{E}_{j+1}^\pm\rangle$ such that the energy leaving the molecule enters the bath:

$$\begin{aligned} &\langle\mathcal{E}_\pm(\varphi_j)|H_{\rm elec}(\varphi_j)|\mathcal{E}_\pm(\varphi_j)\rangle + \langle\mathscr{E}_j^\pm|H_\mathcal{B}|\mathscr{E}_j^\pm\rangle \\ &= \langle\mathcal{E}_\pm(\varphi_j)|H_{\rm elec}(\varphi_{j+1})|\mathcal{E}_\pm(\varphi_j)\rangle + \langle\mathscr{E}_{j+1}^\pm|H_\mathcal{B}|\mathscr{E}_{j+1}^\pm\rangle. \end{aligned} \tag{B22}$$

For simplicity, we assume that $\mathcal{B}$ has only one pair $|\mathscr{E}_j^\pm\rangle$, $|\mathscr{E}_{j+1}^\pm\rangle$ that satisfies condition (B22), for each j. This assumption can be relaxed.

The isometry

$$\bar{U}_{\rm tick} := \sum_{j=0}^{2f-1} \sum_{\mu=\pm} |\mathcal{E}_\mu(\varphi_j)\rangle\langle\mathcal{E}_\mu(\varphi_j)| \otimes |\varphi_{j+1}\rangle\langle\varphi_j| \otimes |\mathscr{E}_{j+1}^\mu\rangle\langle\mathscr{E}_j^\mu| \tag{B23}$$

rotates the molecule while transferring energy from the molecule to the bath. $\bar{U}_{\rm tick}$ preserves the average energy by design: If ρ denotes the initial state of the molecule-and-bath composite, $\mathrm{Tr}\left[\rho(H_{\rm mol}+H_{\mathcal{B}})\right] = \mathrm{Tr}\left[\bar{U}_{\rm tick}\rho\bar{U}_{\rm tick}^{\dagger}(H_{\rm mol}+H_{\mathcal{B}})\right]$.

Three opportunities remain for future work: (i) $\bar{U}_{\rm tick}$ should be elevated from an isometry to a unitary. (ii) The energy conservation should be elevated from average to exact: $\bar{U}_{\rm tick}$ should commute with the global Hamiltonian. Exact conservation might require further use of reference frames. Some thermodynamic-resource-theory works, however, have required only average energy conservation [94]. (iii) The dissipation should be generalized to arbitrary molecule-bath coupling strengths. Suppose that the bath occupies the state $|\mathscr{E}_j^{\pm}\rangle$, being receptive to energy transfer. $\bar{U}_{\rm tick}$ transfers energy deterministically, reflecting strong coupling. But the coupling might be weak in physical reality. The molecule can have some probability < 1 of dissipating even if the bath is in $|\mathscr{E}_j^{\pm}\rangle$. One would adapt the first set-off equation in [91, App. B], attributed to [134], to many-level systems.

Sequence of time steps: Let $\rho_{\rm mol}$ denote the molecule's initial state. The first two time steps evolve the state as

$$\rho_{\rm mol} \mapsto \mathrm{Tr}_{\mathcal{B}}\left[\bar{U}_{\rm tick}\left(\rho_{\rm mol}\otimes\frac{e^{-\beta H_{\mathcal{B}}}}{Z_{\mathcal{B}}}\right)\bar{U}_{\rm tick}^{\dagger}\right] =: \rho'_{\rm mol} \tag{B24}$$

$$\mapsto e^{-iH_{\rm mol}\Delta t}\left(\rho'_{\rm mol}\right)e^{iH_{\rm mol}\Delta t}\,. \tag{B25}$$

These two evolutions are repeated $f-1$ times.

B 3 Simplification and bounding of the Fisher information

We derive Ineq. (16) by simplifying and bounding Eq. (15). Consider the long-time limit, and suppose that $\rho_{01}\neq 0$. The term proportional to $vt_{\rm f}$ dominates Eq. (15), and

$$I_{\rm F} \sim 16v^2t_{\rm f}^2|\mathrm{Re}(\rho_{01})|^2. \tag{B26}$$

The simplified $I_{\rm F}$ depends on the off-diagonal element ρ_{01} of the density matrix relative to the diabatic basis. Furthermore, this $I_{\rm F}$ is proportional to the squared momentum, $(vt_{\rm f})^2$. This proportionality quantifies how underdamping near the avoided crossing generates more coherence than overdamping would generate. The long-time population is well-approximated by the Landau-Zener transition probability, $\rho_{11}\approx\exp\left(-\frac{\pi\lambda^2}{2\hbar v}\right)$ [46]. We approximate the long-time density matrix's off-diagonal elements by neglecting the phase: $\rho_{01}\approx\exp\left(-\frac{\pi\lambda^2}{4\hbar v}\right)\sqrt{1-\exp\left(-\frac{\pi\lambda^2}{2\hbar v}\right)}$. Within the approximate treatment of the avoided crossing, therefore, the final-state coherence in the electronic state is upper-bounded by

$$I_{\rm F}^{+} = 16v^2t_{\rm f}^2e^{-\pi\lambda^2/(2\hbar v)}\left(1-e^{-\pi\lambda^2/(2\hbar v)}\right). \tag{B27}$$

We have bounded a closed system's $I_{\rm F}$. $I_{\rm F}$ is a thermal-operations monotone. Hence any action of the bath results in $I_{\rm F}\big(\rho_{\rm f}^{\rm elec}, H_{\rm LZ}(t_{\rm f})\big) < I_{\rm F}^{+}$.

B 4 Work extraction and injection

Using the resource-theory framework, we show that work can be extracted from postisomerization coherence, if molecules interact and obey indistinguishable-particle statistics. We also calculate the minimal work required to photoexcite the molecule. We use two resource-theory tools: (i) one-shot information theory, which generalizes Shannon information theory to small scales, and (ii) quantum-thermodynamic results about extracting work from coherence.

B 4 i Extracting work from postisomerization coherence

The postisomerization state $\rho_{\rm f}$ can have coherence between unequal-energy electronic levels, $|\mathcal{E}_{\pm}(\pi)\rangle|\varphi{=}\pi\rangle$. Work can be extracted from coherence between degenerate levels, resource-theory results show [93, 111, 135, 136]. We can

generate degenerate-level coherence from unequal-energy coherence, using multiple copies of the system. The work comes from coherence because the extraction preserves the state's energy diagonal.

Consider two molecules that dissipate weakly during isomerization. Having begun in a nearly pure state, the isomers end nearly in some pure state $|\chi\rangle|\varphi{=}\pi\rangle^{\otimes 2}$. The electronic factor has the form

$$\begin{aligned}|\chi\rangle = &\sqrt{p_{--}}|\mathcal{E}_-(\pi), \mathcal{E}_-(\pi)\rangle + \sqrt{p_{-+}}|\mathcal{E}_-(\pi), \mathcal{E}_+(\pi)\rangle \\ &+ \sqrt{p_{+-}}|\mathcal{E}_+(\pi), \mathcal{E}_-(\pi)\rangle + \sqrt{p_{++}}|\mathcal{E}_+(\pi), \mathcal{E}_+(\pi)\rangle.\end{aligned} \tag{B28}$$

One can initiate work extraction by measuring the system's energy, e.g., to ascertain how much work is expected and so to guide instrument calibration. Suppose that (i) the equal-energy eigenstates have equal prefactors, $\sqrt{p_{-+}} = \sqrt{p_{+-}}$, and (ii) the greatest Gibbs-rescaled probability is p_{+-}:

$$\arg\max_{\tilde{\mathcal{E}}} \left\{ p_{\mu\nu} e^{\beta\tilde{\mathcal{E}}} \right\} = \mathcal{E}_+(\pi) + \mathcal{E}_-(\pi). \tag{B29}$$

Suppose, further, that the measurement yields the degenerate energy, $\mathcal{E}_-(\pi) + \mathcal{E}_+(\pi)$. The system is projected onto a pure state, $\frac{1}{\sqrt{2}} [|\mathcal{E}_-(\pi), \mathcal{E}_+(\pi)\rangle + |\mathcal{E}_+(\pi), \mathcal{E}_-(\pi)\rangle]$, in a two-dimensional space. The pure state has more informational value than the same-energy-diagonal mixed state, $\frac{1}{2}[|\mathcal{E}_-(\pi)\rangle\langle\mathcal{E}_-(\pi)| + |\mathcal{E}_+(\pi)\rangle\langle\mathcal{E}_+(\pi)|]$. The pure state can be decohered to the mixed state while the extra value is extracted as work (see Fig. 2 in [111]).

Let us illustrate how a two-molecule state can satisfy the criterion (B29). Though artificial, the illustration demonstrates achievability. Suppose that the molecules occupy a small, symmetric structure. Their real-space wave functions might overlap considerably, rendering the molecules indistinguishable [137]. The molecules would occupy a symmetric or an antisymmetric state, depending on their total spins [137]. Hence the electronic DOFs could occupy an antisymmetric state [137]. Suppose that a Heisenberg Hamiltonian $\propto \boldsymbol{\sigma}\cdot\boldsymbol{\sigma}$ couples the electronic DOFs during photoisomerization. Let the Hamiltonian's proportionality constant be positive. Suppose, further, that the photoisomers thermalize with a $T = 0$ bath. The electronic state cools to the ground state, the singlet $\frac{1}{\sqrt{2}}[|\mathcal{E}_+(\pi), \mathcal{E}_-(\pi)\rangle - |\mathcal{E}_-(\pi), \mathcal{E}_+(\pi)\rangle]$, satisfying Eq. (B29). The photoisomers could decouple quickly after photoisomerizing. The total Hamiltonian would return to $H_{\rm mol} + H_{\rm mol}$ while the state remained a singlet. Work could be extracted from the state's coherence, if an agent acted quickly enough. Granted, the decoupling would cost (positive or negative) work. But that work could, in principle, come from the photoisomers themselves, or from structures to which the photoisomers were attached, rather than from the battery charged later from the coherence.

B 4 ii Minimal work required to photoisomerize

How much work must one invest to excite a molecule from $\exp(-\beta H_{\rm mol})/Z_{\rm mol}$ to $|\psi_1\rangle|\varphi{=}0\rangle$? One might expect an average of about $\mathcal{E}_+(0) - \mathcal{E}_-(0)$. But the single-photon limit invites us to consider the minimal work $W_{\rm min}$ required in any one shot. One-shot work can be calculated in thermodynamic resource theories [66, 95, 103, 134, 138–140]. Calculations rely on one-shot information theory [141–145], which extends Shannon information theory [146] to small scales and few trials.

Work can be defined in terms of a battery [66]. The battery can manifest as an oscillator governed by a Hamiltonian like $H_{\rm laser}$ [68, 75, 93, 95]. A battery performs work while facilitating a system-of-interest transformation from some state ρ to some state ρ'. The work is positive, $\hbar\omega > 0$, if the battery de-excites: $(\rho\otimes|n_\omega\rangle\langle n_\omega|) \mapsto (\rho'\otimes|n_\omega - 1\rangle\langle n_\omega - 1|)$. We regard the light source as consisting of batteries of various gaps $\hbar\omega$ (see Sec. I A).

Consider creating one copy of an arbitrary energy-diagonal system $\big(\mathcal{D}(\rho), H\big)$ from a thermal system $(\exp[-\beta H]/Z, H)$. The minimal work required has been shown to equal

$$W_{\rm min}\big(\mathcal{D}(\rho), H\big) = \frac{1}{\beta} D_{\rm max}\left(\rho || e^{-\beta H}/Z\right) \tag{B30}$$

[66]. The max relative entropy between quantum states ρ and σ is defined as

$$D_{\rm max}(\rho||\sigma) := \log(\min\{c \in \mathbb{R} : \rho \leq c\sigma\}). \tag{B31}$$

We set logarithms to be base-e in this paper. $D_{\rm max}$ is well-defined if the first state's support lies in the second state's: $\mathrm{supp}(\rho) \subseteq \mathrm{supp}(\sigma)$. This entropy quantifies how well ρ and σ can be distinguished in a particular trial of state discrimination [147].

Using these results, we calculate the work required to excite the molecule's thermal state to $|\psi_1\rangle|\varphi{=}0\rangle$. We notate the energy diagonal as

$$\begin{aligned}&\mathcal{D}(|\psi_1\rangle\langle\psi_1| \otimes |\varphi{=}0\rangle\langle\varphi{=}0|) \\ &= \sum_{\mu=\pm} p_\mu |\mathcal{E}_\mu(0)\rangle\langle\mathcal{E}_\mu(0)| \otimes |\varphi{=}0\rangle\langle\varphi{=}0| \, . \end{aligned} \tag{B32}$$

Substituting into Eq. (B30) yields

$$\begin{aligned}&W_{\min}(\mathcal{D}(|\psi_1\rangle\langle\psi_1| \otimes |\varphi{=}0\rangle\langle\varphi{=}0|), H_{\rm mol}) \\ &= \max_{\mu=\pm} \left\{ \mathcal{E}_\mu(0) - \frac{1}{\beta} \log\left(1/p_\mu\right) \right\} - \left(-\frac{1}{\beta} \log Z_{\rm mol} \right) \, . \end{aligned} \tag{B33}$$

The expression maximized over equals a one-shot variation on a free-energy difference: The Helmholtz free energy is defined, in conventional thermodynamics, as $F := E - TS$. The eigenenergy $\mathcal{E}_\mu(0)$ replaces the average energy E. p_μ equals a probability, so $-\log(p_\mu)$ equals a surprisal: Consider preparing $|\psi_1\rangle|\varphi{=}0\rangle$, then measuring the energy. The surprisal quantifies the information you gain, or the surprise you register, upon learning the outcome. Averaging the surprisal over many trials yields the Shannon entropy, $S_{\rm Sh} = -\sum_{\mu=\pm} p_\mu \log p_\mu$. The Shannon entropy is proportional to the thermodynamic entropy S, for equilibrium states. Hence the $-\frac{1}{\beta}\log(1/p_\mu)$ is a one-shot variation on the $-TS$ in F. The equilibrium state $\exp(-\beta H_{\rm mol})/Z_{\rm mol}$ has a free energy of $F = -\frac{1}{\beta}\log Z_{\rm mol}$. Hence the minimal one-shot work has the form (one-shot nonequilibrium free energy) - (equilibrium free energy).

Equation (B33) reduces to the expected formula in a simple case. Suppose that the diabatic state $|\psi_1\rangle|\varphi{=}0\rangle$ exactly equals the energy eigenstate $|\mathcal{E}_+(0)\rangle|\varphi{=}0\rangle$ and that the equilibrium state $e^{-\beta H_{\rm mol}}/Z_{\rm mol}$ exactly equals the energy eigenstate $|\mathcal{E}_-(0)\rangle|\varphi{=}0\rangle$. First, the final-state probabilities become $p_+ = 1$ and $p_- = 0$. Therefore, the maximum evaluates to $\mathcal{E}_+(0)$. Second, the Boltzmann weight $e^{-\beta\mathcal{E}_-(0)}/Z_{\rm mol} = 1$. Therefore, the equilibrium free energy reduces to $-\frac{1}{\beta}\log Z_{\rm mol} = \mathcal{E}_-(0)$. Substituting into Eq. (B33) yields a $W_{\min}$ of $\mathcal{E}_+(0) - \mathcal{E}_-(0)$. The minimal work required to photoexcite the ground *cis* state into the excited *cis* state equals the energy gap.

REFERENCES

[1] C. Jarzynski, Physical Review Letters **78**, 2690 (1997).
[2] G. E. Crooks, Physical Review E **60**, 2721 (1999).
[3] R. Klages, W. Just, and C. Jarzynski, *Nonequilibrium statistical physics of small systems: Fluctuation relations and beyond* (John Wiley & Sons, 2013).
[4] D. Collin *et al.*, Nature **437**, 231 (2005).
[5] E. Trepagnier *et al.*, Proceedings of the National Academy of Sciences **101**, 15038 (2004).
[6] D. Mandal and C. Jarzynski, Proceedings of the National Academy of Sciences **109**, 11641 (2012).
[7] S. Toyabe, T. Sagawa, M. Ueda, E. Muneyuki, and M. Sano, Nature physics **6**, 988 (2010).
[8] J. V. Koski, V. F. Maisi, T. Sagawa, and J. P. Pekola, Physical review letters **113**, 030601 (2014).
[9] A. C. Barato and U. Seifert, Physical review letters **114**, 158101 (2015).
[10] T. R. Gingrich, J. M. Horowitz, N. Perunov, and J. L. England, Physical review letters **116**, 120601 (2016).
[11] A. C. Barato, D. Hartich, and U. Seifert, New Journal of Physics **16**, 103024 (2014).
[12] A. C. Barato and U. Seifert, Physical Review X **6**, 041053 (2016).
[13] M. Nguyen and S. Vaikuntanathan, Proceedings of the National Academy of Sciences **113**, 14231 (2016).
[14] R. Marsland III and J. England, Reports on Progress in Physics **81**, 016601 (2017).
[15] D. H. Waldeck, Chemical Reviews **91**, 415 (1991).
[16] Q. Wang, R. W. Schoenlein, L. A. Peteanu, R. A. Mathies, and C. V. Shank, Science **266**, 422 (1994).
[17] H. D. Bandara and S. C. Burdette, Chemical Society Reviews **41**, 1809 (2012).
[18] S. Hahn and G. Stock, The Journal of Physical Chemistry B **104**, 1146 (2000).
[19] S. Hahn and G. Stock, The Journal of Chemical Physics **116**, 1085 (2002), https://doi.org/10.1063/1.1428344.
[20] W. R. Browne and B. L. Feringa, Nature Nanotechnology **1**, 25 (2006).
[21] A. Kahan, O. Nahmias, N. Friedman, M. Sheves, and S. Ruhman, Journal of the American Chemical Society **129**, 537 (2007).
[22] B. G. Levine and T. J. Martínez, Annu. Rev. Phys. Chem. **58**, 613 (2007).
[23] P. J. M. Johnson *et al.*, The Journal of Physical Chemistry B **121**, 4040 (2017).
[24] O. Strauss, Physiological reviews **85**, 845 (2005).
[25] R. Y. Tsien, Annu. Rev. Biochem **67**, 509 (1998).
[26] G. Vogt, G. Krampert, P. Niklaus, P. Nuernberger, and G. Gerber, Phys. Rev. Lett. **94**, 068305 (2005).
[27] G. Vogt *et al.*, Phys. Rev. A **74**, 033413 (2006).

[28] C. Brif, R. Chakrabarti, and H. Rabitz, New Journal of Physics **12**, 075008 (2010).
[29] V. I. Prokhorenko *et al.*, science **313**, 1257 (2006).
[30] C. Arango and P. Brumer, The Journal of Chemical Physics **138**, 071104 (2013).
[31] T. J. Kucharski *et al.*, Nature Chemistry **6**, 441 (2014).
[32] Y. Zhao and T. Ikeda, *Smart light-responsive materials: azobenzene-containing polymers and liquid crystals* (John Wiley & Sons, 2009).
[33] A. H. Zewail, The Journal of Physical Chemistry **100**, 12701 (1996).
[34] S. Mukamel, Annual review of physical chemistry **51**, 691 (2000).
[35] D. M. Jonas, Annual review of physical chemistry **54**, 425 (2003).
[36] T. A. Oliver, N. H. Lewis, and G. R. Fleming, Proceedings of the National Academy of Sciences , 201409207 (2014).
[37] D. A. Micha, The Journal of Chemical Physics **137**, 22A521 (2012).
[38] A. Kelly and T. E. Markland, The Journal of Chemical Physics **139**, 014104 (2013).
[39] A. Montoya-Castillo, T. C. Berkelbach, and D. R. Reichman, The Journal of Chemical Physics **143**, 194108 (2015).
[40] W. H. Miller, The Journal of Chemical Physics **53**, 3578 (1970).
[41] M. Ben-Nun and T. J. Martínez, The Journal of Chemical Physics **108**, 7244 (1998).
[42] M. Topaler and N. Makri, The Journal of Physical Chemistry **100**, 4430 (1996).
[43] R. Kapral and G. Ciccotti, The Journal of Chemical Physics **110**, 8919 (1999).
[44] A. McLachlan, Molecular Physics **8**, 39 (1964).
[45] J. C. Tully, The Journal of Chemical Physics **93**, 1061 (1990).
[46] A. Nitzan, *Chemical dynamics in condensed phases: relaxation, transfer and reactions in condensed molecular systems* (Oxford university press, 2006).
[47] J. C. Tully, The Journal of Chemical Physics **137**, 22A301 (2012).
[48] A. J. Schile and D. T. Limmer, arXiv:1809.03501 (2018).
[49] B. Coecke, T. Fritz, and R. W. Spekkens, Information and Computation **250**, 59 (2016), Quantum Physics and Logic.
[50] E. Chitambar and G. Gour, ArXiv e-prints (2018), 1806.06107.
[51] R. Horodecki, P. Horodecki, M. Horodecki, and K. Horodecki, Rev. Mod. Phys. **81**, 865 (2009).
[52] S. J. van Enk, Phys. Rev. A **71**, 032339 (2005).
[53] J. A. Vaccaro, F. Anselmi, H. M. Wiseman, and K. Jacobs, Phys. Rev. A **77**, 032114 (2008).
[54] S. D. Bartlett, T. Rudolph, R. W. Spekkens, and P. S. Turner, New J. Phys. **8**, 58 (2006).
[55] S. D. Bartlett, T. Rudolph, and R. W. Spekkens, Rev. Mod. Phys. **79**, 555 (2007).
[56] G. Gour and R. W. Spekkens, New Journal of Physics **10**, 033023 (2008).
[57] I. Marvian and R. W. Spekkens, New Journal of Physics **15**, 033001 (2013).
[58] T. Baumgratz, M. Cramer, and M. B. Plenio, Phys. Rev. Lett. **113**, 140401 (2014).
[59] A. Winter and D. Yang, Phys. Rev. Lett. **116**, 120404 (2016).
[60] E. Chitambar and G. Gour, Phys. Rev. Lett. **117**, 030401 (2016).
[61] V. Veitch, S. A. H. Mousavian, D. Gottesman, and J. Emerson, New Journal of Physics **16**, 013009 (2014).
[62] E. H. Lieb and J. Yngvason, Physics Reports **310**, 1 (1999).
[63] D. Janzing, P. Wocjan, R. Zeier, R. Geiss, and T. Beth, Int. J. Theor. Phys. **39**, 2717 (2000).
[64] M. Horodecki *et al.*, Phys. Rev. Lett. **90**, 100402 (2003).
[65] F. G. S. L. Brandão, M. Horodecki, J. Oppenheim, J. M. Renes, and R. W. Spekkens, Physical Review Letters **111**, 250404 (2013).
[66] M. Horodecki and J. Oppenheim, Nat. Commun. **4**, 2059 (2013).
[67] G. Gour, M. P. Mueller, V. Narasimhachar, R. W. Spekkens, and N. Y. Halpern, Physics Reports **583**, 1 (2015), The resource theory of informational nonequilibrium in thermodynamics.
[68] N. Yunger Halpern, Journal of Physics A: Mathematical and Theoretical **51**, 094001 (2018).
[69] V. Narasimhachar and G. Gour, Nature Communications **6**, 7689 (2015).
[70] M. Lostaglio, D. Jennings, and T. Rudolph, Nature Communications **6**, 6383 (2015).
[71] W. Pauli, *Handbuch der Physick* (Springer, Berlin, 1933), pp. 24 : 83–272.
[72] W. Pauli, *Encyclopedia of Physics* (Springer, Berlin, 1958), p. 1 : 60.
[73] R. P. Feynman, Foundations of Physics **16**, 507 (1986).
[74] N. Margolus, Annals of the New York Academy of Sciences **480**, 487.
[75] J. Åberg, Phys. Rev. Lett. **113**, 150402 (2014).
[76] A. S. L. Malabarba, A. J. Short, and P. Kammerlander, New Journal of Physics **17**, 045027 (2015).
[77] M. F. Frenzel, D. Jennings, and T. Rudolph, New Journal of Physics **18**, 023037 (2016).
[78] M. P. Woods, R. Silva, and J. Oppenheim, ArXiv e-prints (2016), 1607.04591.
[79] P. Erker *et al.*, Phys. Rev. X **7**, 031022 (2017).
[80] M. P. Woods, R. Silva, G. Pütz, S. Stupar, and R. Renner, ArXiv e-prints (2018), 1806.00491.
[81] O. Pusuluk, T. Farrow, C. Deliduman, K. Burnett, and V. Vedral, Proceedings of the Royal Society of London A: Mathematical, Physical and Engineering Sciences **474** (2018).
[82] S. Hahn and G. Stock, The Journal of Physical Chemistry B **104**, 1146 (2000).
[83] J. E. Kim, M. J. Tauber, and R. A. Mathies, Biophysical Journal **84**, 2492 (2003).
[84] I. Burghardt and J. T. Hynes, The Journal of Physical Chemistry A **110**, 11411 (2006).
[85] G. Stock and M. Thoss, Advances in chemical physics **131**, 243 (2005).
[86] E. Brunk and U. Rothlisberger, Chemical reviews **115**, 6217 (2015).

[87] G. Worth, H.-D. Meyer, H. Köppel, L. Cederbaum, and I. Burghardt, International Reviews in Physical Chemistry **27**, 569 (2008).
[88] P. E. Videla, A. Markmann, and V. S. Batista, Journal of Chemical Theory and Computation **14**, 1198 (2018).
[89] M. Sala and D. Egorova, Chemical Physics **515**, 164 (2018), Ultrafast Photoinduced Processes in Polyatomic Molecules:Electronic Structure, Dynamics and Spectroscopy (Dedicated to Wolfgang Domcke on the occasion of his 70th birthday).
[90] M. Lostaglio, K. Korzekwa, D. Jennings, and T. Rudolph, Physical Review X **5**, 021001 (2015).
[91] M. Lostaglio, Á. M. Alhambra, and C. Perry, Quantum **2**, 52 (2018).
[92] S. Bedkihal, J. Vaccaro, and S. Barnett, ArXiv e-prints (2016), 1603.00003.
[93] P. Skrzypczyk, A. J. Short, and S. Popescu, arXiv:1302.2811 (2013).
[94] P. Skrzypczyk, A. J. Short, and S. Popescu, Nature Communications **5**, 4185 (2014).
[95] N. Yunger Halpern and J. M. Renes, Phys. Rev. E **93**, 022126 (2016).
[96] L. Masanes and J. Oppenheim, ArXiv e-prints (2014), 1412.3828.
[97] I. Marvian and R. W. Spekkens, Phys. Rev. A **90**, 062110 (2014).
[98] E. Ruch, Theoretica Chimica Acta **19**, 225 (1975).
[99] E. Ruch, Theoretica Chimica Acta **38**, 167 (1975).
[100] E. Ruch and B. Lesche, J. Chem. Phys. **69**, 393 (1978).
[101] E. Ruch and A. Mead, Theoretica Chimica Acta **41**, 95 (1976).
[102] E. Ruch, R. Schranner, and T. H. Seligman, The Journal of Chemical Physics **69**, 386 (1978).
[103] D. Egloff, O. C. O. Dahlsten, R. Renner, and V. Vedral, New Journal of Physics **17**, 073001 (2015).
[104] A. W. Marshall, I. Olkin, and B. C. Arnold, *Inequalities: theory of majorization and its applications* (Springer, 2010).
[105] M. Thoss and H. Wang, Chemical Physics **322**, 210 (2006).
[106] G. Gour, D. Jennings, F. Buscemi, R. Duan, and I. Marvian, Nature Communications **9**, 5352 (2018).
[107] P. Ao *et al.*, Physical review letters **62**, 3004 (1989).
[108] K. Saito, M. Wubs, S. Kohler, Y. Kayanuma, and P. Hänggi, Physical Review B **75**, 214308 (2007).
[109] L. Arceci, S. Barbarino, R. Fazio, and G. E. Santoro, Physical Review B **96**, 054301 (2017).
[110] R. K. Malla, E. Mishchenko, and M. Raikh, Physical Review B **96**, 075419 (2017).
[111] H. Kwon, H. Jeong, D. Jennings, B. Yadin, and M. S. Kim, Phys. Rev. Lett. **120**, 150602 (2018).
[112] X. N. Feng and L. F. Wei, Scientific Reports **7**, 15492 (2017).
[113] G. Ashkenazi, R. Kosloff, and M. A. Ratner, Journal of the American Chemical Society **121**, 3386 (1999).
[114] J. Yang, S. Pang, and A. N. Jordan, Physical Review A **96**, 020301 (2017).
[115] E. Shimshoni and Y. Gefen, Annals of Physics **210**, 16 (1991).
[116] R. S. Whitney, M. Clusel, and T. Ziman, Phys. Rev. Lett. **107**, 210402 (2011).
[117] G. S. Engel *et al.*, Nature **446**, 782 (2007).
[118] M. Sarovar, A. Ishizaki, G. R. Fleming, and K. B. Whaley, Nature Physics **6**, 462 EP (2010), Article.
[119] H.-G. Duan *et al.*, Proceedings of the National Academy of Sciences **114**, 8493 (2017), http://www.pnas.org/content/114/32/8493.full.pdf.
[120] H. C. H. Chan, O. E. Gamel, G. R. Fleming, and K. B. Whaley, Journal of Physics B: Atomic, Molecular and Optical Physics **51**, 054002 (2018).
[121] A. E. Jailaubekov *et al.*, Nature Materials **12**, 66 EP (2012), Article.
[122] G. M. Akselrod *et al.*, Nano Letters **14**, 3556 (2014).
[123] R. H. Gilmore, E. M. Lee, M. C. Weidman, A. P. Willard, and W. A. Tisdale, Nano letters **17**, 893 (2017).
[124] J. Lin *et al.*, Nature materials **17**, 261 (2018).
[125] D. A. Strubbe and J. C. Grossman, Journal of Physics: Condensed Matter **31**, 034002 (2018).
[126] N. Yunger Halpern, *Toward Physical Realizations of Thermodynamic Resource Theories* (Springer International Publishing, Cham, 2017), pp. 135–166.
[127] N. Lörch, C. Bruder, N. Brunner, and P. P. Hofer, Quantum Science and Technology **3**, 035014 (2018).
[128] Z. Holmes, S. Weidt, D. Jennings, J. Anders, and F. Mintert, ArXiv e-prints (2018), 1806.11256.
[129] Á. M. Alhambra, M. Lostaglio, and C. Perry, ArXiv e-prints (2018), 1807.07974.
[130] J. R. Johansson, P. D. Nation, and F. Nori, Computer Physics Communications **184**, 1234 (2013).
[131] A. Kitaev, D. Mayers, and J. Preskill, Phys. Rev. A **69**, 052326 (2004).
[132] L. Mandel and E. Wolf, *Optical Coherence and Quantum Optics* (Cambridge UP, 1995).
[133] J. C. Light, I. P. Hamilton, and J. V. Lill, The Journal of Chemical Physics **82**, 1400 (1985), https://doi.org/10.1063/1.448462.
[134] J. Åberg, Nat. Commun. **4**, 1925 (2013).
[135] P. Skrzypczyk, A. J. Short, and S. Popescu, Nature Communications **5**, 4185 (2014).
[136] K. Korzekwa, M. Lostaglio, J. Oppenheim, and D. Jennings, New Journal of Physics **18**, 023045 (2016).
[137] M. P. A. Fisher and L. Radzihovsky, Proceedings of the National Academy of Sciences **115**, E4551 (2018), http://www.pnas.org/content/115/20/E4551.full.pdf.
[138] L. Del Rio, J. Åberg, R. Renner, O. Dahlsten, and V. Vedral, Nature **474**, 61 (2011).
[139] J. M. Renes, The European Physical Journal Plus **129**, 153 (2014).
[140] P. Faist, M. Berta, and F. Brandão, ArXiv e-prints (2018), 1807.05610.
[141] R. Renner, *Security of Quantum Key Distribution*, PhD thesis, PhD Thesis, 2005, 2005.

[142] N. Datta, IEEE T. Inform. Theory **55**, 2816 (2009).
[143] M. Berta, *Quantum Side Information: Uncertainty Relations, Extractors, Channel Simulations*, PhD thesis, ETH Zürich, 2013.
[144] F. Leditzky, *Relative entropies and their use in quantum information theory*, PhD thesis, U. of Cambridge, 2016.
[145] M. M. Wilde, *Quantum Information Theory*, 2 ed. (Cambridge University Press, 2017).
[146] C. E. Shannon, Bell Syst. Tech. J. **47**, 379 (1948).
[147] A. J. P. Garner, *One-shot information-theoretical approaches to fluctuation theorems* (Springer, 2018), .